10/5/22/89 98(1)

SANDIA REPORT

SAND88—2710 • UC—126
Unlimited Release
Printed November 1988

Modified Local Similarity for Natural Convection Along a Nonisothermal Vertical Flat Plate Including Stratification

Stephen W. Webb

MASTER

SF2900Q(8-81)

MODIFIED LOCAL SIMILARITY FOR NATURAL CONVECTION ALONG A NONISOTHERMAL VERTICAL FLAT PLATE INCLUDING STRATIFICATION

Stephen W. Webb
SPR Geotechnical Division 6257
Sandia National Laboratories
Albuquerque, New Mexico   87185

Abstract

Natural convection along vertical surfaces occurs in the oil filled caverns in the Strategic Petroleum Reserve (SPR). These caverns are located in large salt domes where the geothermal temperature difference over the cavern height of up to 2000 feet can be 30°F with the hotter salt at the bottom of the cavern. Due to the coupling of the heat transfer between the salt and the fluids in the cavern, heat transfer to the oil and the resulting natural convection can occur during the entire anticipated storage period of up to 30 years. The wall and fluid conditions are spatially nonuniform due to the geothermal temperature difference and fluid temperature stratification.

The Modified Local Similarity (MLS) method has been developed and applied to natural convection along a vertical flat plate with variable surface conditions and temperature stratification for application to natural convection in SPR caverns. The MLS method explicitly conserves energy along the plate. The boundary layer velocity and temperature profiles are evaluated by the local similarity method with appropriate values of the similarity parameters. The MLS method is a significant improvement to the local similarity approach and is a useful approximate tool for analyzing natural convection on vertical surfaces for nonsimilar conditions.

Table of Contents

I. Introduction

Natural convection along vertical surfaces occurs in the oil filled caverns in the Strategic Petroleum Reserve (SPR). These caverns are located in large salt domes where the geothermal temperature difference over the cavern height of up to 2000 feet can be 30°F or more. The hotter salt is located at the bottom of the cavern; this configuration will cause natural convection in the enclosed fluids as a result of buoyancy forces. Since the heat transfer between the salt and the fluids in the cavern is coupled, heat transfer to the oil and the resulting natural convection can occur during the entire anticipated storage period of up to 30 years. SPR cavern wall conditions are nonuniform due to the geothermal temperature difference. In addition, the fluid temperature is nonuniform owing to the thermal stratification of the oil. Thus, the wall conditions and the ambient fluid temperature are both variable.

The methods in general use for the analysis of natural convection are the integral, similarity, local nonsimilarity, and finite difference approaches. In addition, approximate methods have been developed by Raithby, et al. (1975, 1977, 1978) and by Lee and Yovanovich (1987, 1988). Each of these methods is discussed below.

The integral method has been used by Sparrow (1955) for certain prescribed variations of wall temperature and wall heat flux. While the results compare well to similarity solutions for constant wall heat flux, no comparison for nonuniform wall temperature or heat flux is known. The integral results reported by Sparrow (1955) will be compared to the results of other methods in this report for the applicable cases. In general, the weakness of the integral approach is that the velocity and temperature profiles have to be assumed. While the assumed profiles may be adequate for normal conditions, the effect of changes in the boundary conditions are not reflected in the profiles. In addition, acceptable profiles for turbulent flow conditions are not available.

The similarity method is a powerful boundary layer approach. In this method, the boundary layer partial differential equations (PDEs) are reduced to ordinary differential equations (ODEs) through the introduction of similarity variables. Unlike the PDE set which has to be solved for each location along the plate, the ODE set only has to be solved once for a given set of parameters. The resulting solution is valid along the entire plate. Unfortunately, similarity solutions only exist for a restricted number of wall temperature variations and fluid temperature stratification.

As an approximate solution to other wall and fluid temperature variations, the similarity method can be applied locally; this approach is called the local similarity approach. The approach allows for rapid, though approximate, evaluation of natural convection phenomena. However, the values of the similarity variables are chosen based on the type of boundary conditions imposed without regard to the variation of these conditions along the plate. As shown by Sparrow and Gregg (1958), this technique may give poor results. They applied similarity results from an

1

isothermal wall to a variable wall temperature case. The resulting total heat transfer for the plate was significantly in error including cases where the direction of heat transfer was incorrect. Other applications of the local similarity approach (Kao, et al. (1977)) have shown large errors in certain cases.

Local nonsimilarity methods based on the work of Sparrow, et al. (1970, 1971) and Minkowycz and Sparrow (1974) have been used for natural convection as presented by Kao (1976) for variable wall conditions. Chen and Eichhorn (1976) used this approach for a constant temperature wall in a variable temperature fluid. In general, the local nonsimilarity results compare well with data and with the results from numerical calculations.

Finite difference procedures are also available as exemplified by the methods presented by Cebeci and Bradshaw (1984). Results from a numerical approach using finite differences have been given by Kao, et al. (1977) for variable wall temperature and wall heat flux cases. The finite difference approach is considered to be the most accurate technique for the analysis of natural convection boundary layer flow.

Approximate methods have been proposed by Raithby, et al. (1975, 1977, 1978) and by Lee and Yovanovich (1987, 1988). Neither of these methods were considered for use in SPR since neither method reduces the similarity solutions for similar boundary conditions. Differences of up to 20% are noted by Raithby and Hollands (1978) when their method is compared to similarity solutions. The method of Lee and Yovanovich (1987, 1988) shows similar differences and has the added disadvantage of a complicated form.

Analysis of natural convection in SPR caverns involves highly turbulent conditions with Rayleigh numbers of up to 10^{16} and long transient times of up to 30 years (Webb (1988)). Therefore, finite difference and local nonsimilarity methods are impractical due to long estimated computing times which result from the need to recalculate the boundary layer results each time step. The integral method could be used for SPR, although the assumed profiles are a problem, especially for turbulent flow conditions. The wall and fluid temperature variations preclude direct use of the similarity solutions. The local similarity method would be appropriate for SPR in that the boundary layer results can be tabulated for use at each time step; therefore, the answers do not need to be redone each time step and the resulting calculations would be fast. The problem, however, is that the errors in heat transfer rates, including the direction of heat flow, can be significant even for simple cases.

If the heat flow or energy conservation problems noted for the local similarity approach can be corrected, the method would be ideal for SPR use. The present study corrects this problem by modifying the local similarity approach to explicitly conserve energy as the boundary layer develops along the surface. This Modified Local Similarity (MLS) approach is developed and compared to results from other methods in this report. The method has been used in the development of the SPR velocity model as summarized by Webb (1988).

2

II. Formulation

Consider natural convection boundary layer flow along a flat plate as depicted in Figure 1. The boundary layer energy equation can be integrated along the plate using the local boundary layer velocity and temperature profiles. For the present study, the boundary layer profiles are calculated by the local similarity method. The local similarity method has two parameters which are mathematical descriptions of the temperature variation along the plate and in the surrounding fluid. In addition to being mathematical parameters, these variables have physical significance in the boundary layer problem with regard to overall conservation of energy. The global energy conservation equation can be written in terms of the local similarity parameters to ascertain their equivalent values for nonsimilar conditions. The global energy equation and the evaluation of the boundary layer profiles are detailed below.

A. Global Energy Equation

The boundary layer velocity and temperature profiles along a plate will vary with distance x. Considering conservation of energy per unit width of the plate as depicted in Figure 2,

$$\dot{m}_1 \, c_p \, \bar{T}_1 \; + \; \bar{q}'' \, \Delta x \; + \; (\dot{m}_2 - \dot{m}_1) \, c_p \, T_f^*$$
$$= \; \dot{m}_2 \, c_p \, \bar{T}_2 \tag{1}$$

or

$$\dot{m}_1 \, c_p \, (\bar{T}_1 - T_f^*) \; + \; \bar{q}_2'' \, \Delta x \; = \; \dot{m}_2 \, c_p \, (\bar{T}_2 - T_f^*) \tag{2}$$

where

$$\bar{q}_2'' \; = \; \frac{1}{\Delta x} \int_{x_1}^{x_2} q'' \, dx \tag{3}$$

and T_f^* is the average temperature of the fluid entrained into or ejected from the boundary layer. Note that the fluid specific heat, c_p, is assumed to be constant.

The average temperature of the entrained or ejected fluid will be assumed to be equal to the local environmental fluid temperature for this analysis. The velocity boundary layer thickness is larger than the thermal boundary layer for Prandtl number fluids of order 1.0 and higher, so any fluid exchange will be at the environmental temperature if local similarity
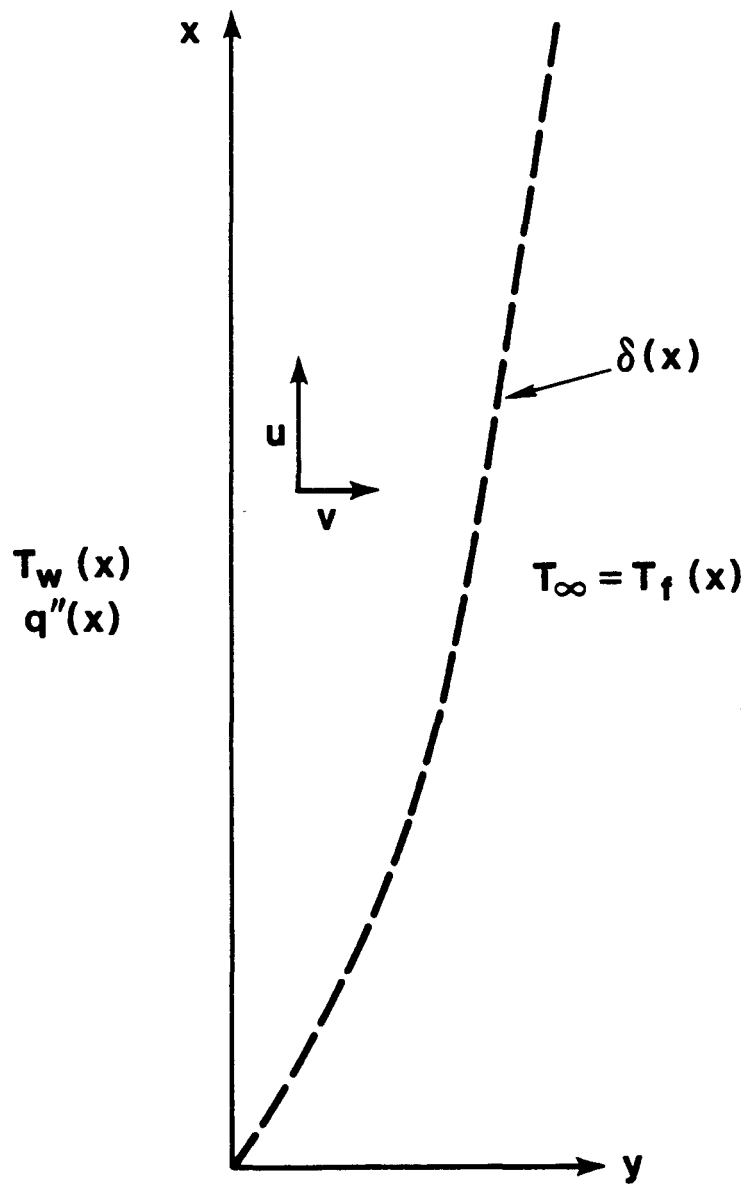
Figure 1. Boundary layer coordinates.

$$(\dot{m}_2 - \dot{m}_1)\, c_p T_f^*$$

$$\dot{m}_1 c_p \overline{T}_1 \longrightarrow$$

$$\longrightarrow \dot{m}_2 c_p \overline{T}_2$$

$$\longrightarrow x$$

$$x_1 \qquad q'' \Delta x \qquad x_2$$

$$\Delta x$$
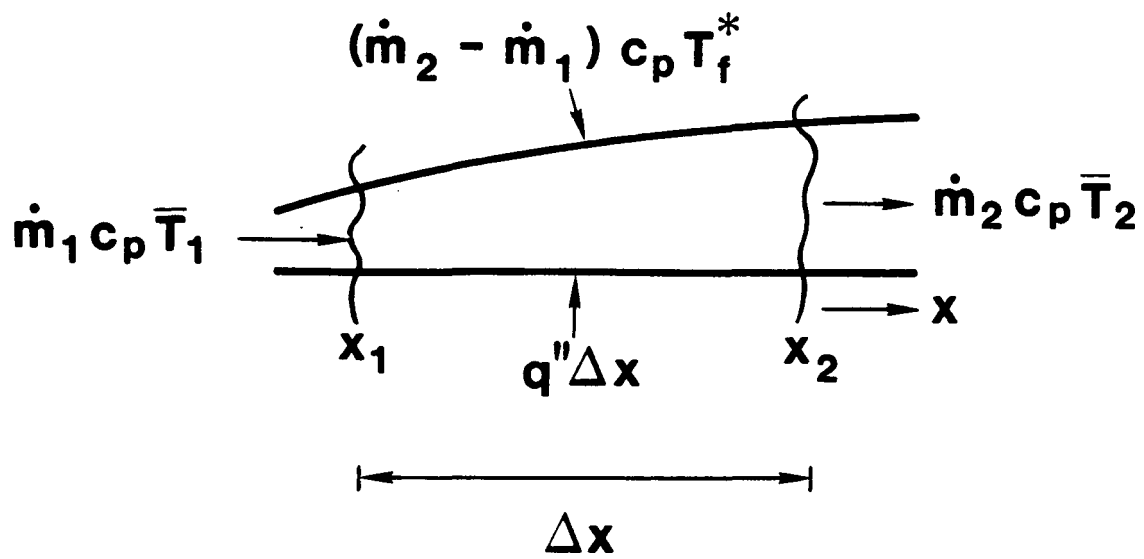
Figure 2. Boundary layer global energy conservation.

is assumed. This assumption breaks down for low Prandtl number fluids such as liquid metals where the similarity solution gives a larger thermal boundary layer than velocity boundary layer (Gebhart (1985)).

The average boundary layer temperature, $\bar{T}$, is the fluid temperature at that location plus the average difference in temperature of the convected fluid over the environmental value, or

$$\bar{T} = T_f(x) + \frac{\int u \, (T - T_f(x)) \, dy}{\int u \, dy} . \tag{4}$$

Combining the above equations results in

$$\dot{m}_1 \, c_p \, (\bar{T}_1 - T_f^*) + \bar{q}_2'' \, \Delta x$$

$$= \dot{m}_2 \, c_p \, (T_{f_2} - T_f^* + \frac{\int u \, (T - T_f(x)) \, dy}{\int u \, dy}) . \tag{5}$$

The above equation is general; any restrictions as to the orientation, etc. are from evaluation of the boundary layer parameters. Knowing the conditions at location 1, the wall heat flux, and the environmental fluid temperature, the above expression can be easily evaluated if the boundary layer velocity and temperature profiles are known. For this study, these profiles will be based on local similarity as discussed in the next section.

B. Boundary Layer Profiles

The boundary layer profiles for use in the global energy equation will be evaluated for laminar natural convection over a nonisothermal vertical flat plate in a variable temperature fluid medium. Invoking the Boussinesq approximation with otherwise constant properties and neglecting viscous dissipation and the pressure-work term, the steady-state conservation equations are (Jaluria (1980))

Continuity

$$\frac{\partial u}{\partial x} + \frac{\partial v}{\partial y} = 0 \tag{6}$$

x-Momentum

$$u \frac{\partial u}{\partial x} + v \frac{\partial u}{\partial y} = g \beta (T - T_f(x)) + \nu \frac{\partial^2 u}{\partial y^2} \tag{7}$$

Energy

$$u \frac{\partial T}{\partial x} + v \frac{\partial T}{\partial y} = \alpha \frac{\partial^2 T}{\partial y^2}. \tag{8}$$

The above conservation equations can be integrated across the boundary layer from y=0 (wall) to y=∞ (environment). Since the velocity v is 0. at y=0. and at y=∞, the integration results in the following (Jaluria (1980))

Momentum

$$\frac{d}{dx} \int u^2 \, dy = g \beta \int (T - T_f(x)) \, dy - \nu \left. \frac{\partial u}{\partial y} \right|_w \tag{9}$$

Energy

$$\frac{d}{dx} \int u (T - T_f(x)) \, dy + \frac{dT_f}{dx} \int u \, dy = - \alpha \left. \frac{\partial T}{\partial y} \right|_w \tag{10}$$

where the second term on the LHS of the energy equation accounts for temperature stratification of the environmental fluid. The continuity equation has been used in the development of the above integrated equations.

Two energy equations are considered in the present analysis. The first energy equation is the global energy equation (5), which is concerned with the energy in the boundary layer as it grows along the plate with respect to x. The second energy equation is the local energy equation (10)

which is related to the energy in the boundary layer at location x only. For energy conservation, both equations must be satisfied. The global energy equation must conserve all the energy added to the boundary layer up to the location x, and the local energy equation must conserve the energy added to the fluid from the wall at location x.

In the present analysis, similarity variables will be used to rewrite the two energy equations. These equations will then be combined to lead to relationships for the similarity variables that must be satisfied for global and local energy conservation.

According to Sparrow and Gregg (1958) and Yang (1960), similarity only exists for two specific distributions of the temperature difference between the wall and the fluid: the power-law and the exponential distributions. In each case, any variation in the fluid temperature must be of the same form as the wall to fluid temperature difference. Since the two distributions lead to different results, each will be discussed separately.

1. Power-Law Distribution

For the power-law distribution, the temperature difference between the wall and fluid is a function of the distance x to a power, or

$$\Delta T(x) = T_w(x) - T_f(x) = N\, x^n. \tag{11}$$

For similarity, the fluid temperature variation must be of the same form, or (Jaluria (1980))

$$T_f(x) - T_r = \frac{J\,N}{4\,n}\, x^n = \frac{J}{4\,n}\, \Delta T(x) \tag{12}$$

where the reference temperature, T_r, is the fluid temperature at $x = 0$. If the fluid temperature is constant, J is equal to 0.

The stream function and similarity variables for this case are (Gebhart and Mollendorf (1969))

$$\psi = 4\left(\frac{Gr_x}{4}\right)^{1/4} \nu\, f(\eta) \tag{13}$$

$$\eta = \left(\frac{Gr_x}{4}\right)^{1/4} \frac{y}{x} \tag{14}$$

$$\theta(\eta) = \frac{T - T_f(x)}{T_w(x) - T_f(x)} \tag{15}$$

where

$$Gr_x = \frac{g\,\beta\, x^3\, (T_w(x) - T_f(x))}{\nu^2} \tag{16}$$

and the fluid velocity in the x direction becomes

$$u = \frac{\partial \psi}{\partial y} = \frac{\partial \psi}{\partial \eta}\, \frac{\partial \eta}{\partial y}$$

$$= \frac{2\,\nu}{x}\, Gr_x^{1/2}\, f'. \tag{17}$$

The boundary layer partial differential equations (6)-(8) reduce to a set of coupled ordinary differential equations when the above similarity variables are imposed. For the power-law distribution, the local similarity form of these equations is (Jaluria (1980))

$$f''' + (n + 3) f f'' - 2 (n + 1) f'^2 + \theta = 0 \qquad (18)$$

$$\frac{\theta''}{Pr} + (n + 3) f \theta' - 4 n f' \theta - J f' = 0 \qquad (19)$$

with the appropriate boundary conditions. These equations have been solved in the present study by the finite difference method since the traditional shooting method was unreliable. This method is summarized by Webb (1989).

The first term to be evaluated for substitution into the global energy equation (5) is the difference between the fluid temperature at location 2 and T_f^*. Expressing the fluid temperature difference in terms of the similarity parameter J gives

$$T_{f_2} - T_f^* = \frac{J N}{4 n} (x_2^n - x^{*n}). \qquad (20)$$

N can be evaluated at location x_2, and the above equation can be rewritten as

$$T_{f_2} - T_f^* = \frac{J \Delta T_2}{4 n} (1 - (\frac{x^*}{x_2})^n). \qquad (21)$$

Using the similarity parameters defined above along with equation (21), the global energy equation (5) becomes

$$\dot{m}_1 c_p (\bar{T}_1 - T_f^*) + \bar{q}_2'' \Delta x$$

$$= \dot{m}_2 c_p (\frac{J}{4 n} (1 - (\frac{x^*}{x_2})^n) + \frac{\int f' \theta \, d\eta}{\int f' \, d\eta}) \Delta T_2. \qquad (22)$$

Expressions for the mass flow rate and the temperature difference at location 2 will now be developed. The mass flow rate per unit width can be expressed in terms of the local similarity variables as

$$\dot{m} = \rho \bar{u} A / W = \rho \bar{u} \delta$$

$$= \rho \frac{2 \nu}{x} Gr_x^{1/2} \frac{\int f' \, d\eta}{\eta_\infty} \eta_\infty x (\frac{Gr_x}{4})^{-1/4}$$

10

$$- 4 \mu \int f' \, d\eta \; (\frac{g \, \beta}{4\nu^2})^{1/4} \; x^{3/4} \; \Delta T^{1/4}. \tag{23}$$

The heat flux relationship

$$q'' = - k \left. \frac{\partial T}{\partial y} \right|_w$$

$$= - k \, \theta'_w \; (\frac{g \, \beta}{4\nu^2})^{1/4} \; \Delta T^{5/4} \; x^{-1/4} \tag{24}$$

can be used to get the temperature difference as a function of x, or

$$\Delta T^{5/4} = (\frac{q''}{- k \, \theta'_w}) \; (\frac{g \, \beta}{4\nu^2})^{-1/4} \; x^{1/4}. \tag{25}$$

Note that for a similarity solution, the dimensionless wall temperature gradient, θ'_w, is constant for all x values, and the heat flux variation can be written as

$$q'' \; \alpha \; \Delta T^{5/4} \; x^{-1/4} \; \alpha \; x^{5n/4} \; x^{-1/4} \; \alpha \; x^{(5n-1)/4} \quad . \tag{26}$$

Using equation (25), the mass flow rate equation can be rewritten as

$$\dot{m} = 4 \mu \int f' \, d\eta \; (\frac{g \, \beta}{4\nu^2})^{0.2} \; x^{0.8} \; (\frac{q''}{- k \, \theta'_w})^{0.2} \tag{27}$$

and the global energy equation (22) then becomes

$$\dot{m}_1 \, c_p \, (\bar{T}_1 - T_f^*) \; + \; \bar{q}_2'' \, \Delta x$$

$$= 4 \, Pr \int f' \, d\eta \; (\frac{q_2''}{- \theta'_w})$$

$$(\frac{J}{4 \, n} \, (1 - (\frac{x^*}{x_2})^n) + \frac{\int f' \theta \, d\eta}{\int f' \, d\eta}) \; x_2 . \tag{28}$$

The same similarity variables can be used in the integrated local boundary layer equations (9) and (10) resulting in the following equations for the boundary layer quantities

11

Momentum

$$(5 + 3n) \int f'^2 \, d\eta - \int \theta \, d\eta - f''_w \tag{29}$$

Energy

$$(5n + 3) \int f' \theta \, d\eta = - \frac{\theta'_w}{Pr} - J \int f' \, d\eta . \tag{30}$$

These relationships are a measure of the shape of the velocity and temperature boundary layer profiles and are useful for checking the accuracy of the numerical solution of the local similarity equations. They are also helpful if numerical fits are generated to some of the boundary layer integrals as these expressions can be used to ensure consistency among the various parameters.

Rearranging the local boundary layer energy equation (30) and substituting it into the global energy equation (28) results in

$$(\dot{m}_1 \, c_p \, (\bar{T}_1 - T_f^*) + \bar{q}_2'' \, \Delta x) \, / \, (q_2'' \, x_2)$$

$$= \frac{\dfrac{J}{n} \, (1 - (\dfrac{x^*}{x_2})^n) + 4 \int f' \, \theta \, d\eta \, / \int f' \, d\eta}{J + (5n + 3) \int f' \, \theta \, d\eta \, / \int f' \, d\eta} . \tag{31}$$

The ratio of the first terms in the numerator and denominator on the RHS and of the second terms on the RHS must both be equal to the LHS. For the second terms,

$$\frac{4}{5n + 3} = (\dot{m}_1 \, c_p \, (\bar{T}_1 - T_f^*) + \bar{q}_2'' \, \Delta x) \, / \, (q_2'' \, x_2) \tag{32}$$

or,

$$n = \frac{1}{5} \, [4 \, q_2'' \, x_2 / \, (\dot{m}_1 \, c_p \, (\bar{T}_1 - T_f^*) + \bar{q}_2'' \, \Delta x) - 3] . \tag{33}$$

Similarly, making use of equation (32), the first terms give

$$x^* = x_2 \, [1 - \frac{4n}{(5n + 3)}]^{1/n} . \tag{34}$$

If x_1 is taken to be at the leading edge of the plate ($x_1=0.$) with no initial mass flow rate, then $\Delta x=x_2$, and the above equation set simplifies considerably to

12

$$n = \frac{1}{5} [4 \, q_2'' / \bar{q}_2'' - 3].$$ (35)

The value of the similarity parameter n is just a function of the ratio of the local to the average heat flux up to that point. The fluid temperature evaluated at x^* is that required for energy conservation.

Surprisingly, the stratification parameter, J, is independent of global conservation of energy. Instead, the value of J is determined by the local value of the heat flux, q_2''. Equating the conservation of energy equations (2) and (33) gives

$$\dot{m}_2 \, c_p \, (\bar{T}_2 - T_f^*) = \frac{4}{(5n + 3)} \, q_2'' \, x_2$$ (36)

where the values on the RHS are known. Expanding the LHS of the above equation results in the expression

$$\dot{m}_2 \, c_p \, (\frac{\int f' \theta \, d\eta}{\int f' \, d\eta} \Delta T_2 + T_{f_2} - T_f^*) = \frac{4}{(5n + 3)} \, q_2'' \, x_2.$$ (37)

This equation includes the effect of temperature stratification on the local energy balance. Using the equations developed above for $\dot{m}$ and ΔT, the above equation can be written as

$$A_1 \frac{\int f' \, d\eta}{(- \theta_w')^{0.2}} (A_2 \frac{\int f' \theta \, d\eta}{\int f' \, d\eta \, (- \theta_w')^{0.8}} + T_{f_2} - T_f^*) = A_3$$ (38)

where

$$A_1 = 4 \, c_p \, \mu \, (\frac{g \, \beta}{4\nu^2})^{0.2} \, x_2^{0.8} \, (\frac{q_2''}{k})^{0.2}$$ (39)

$$A_2 = (\frac{g \, \beta}{4\nu^2})^{-0.2} \, x_2^{0.2} \, (\frac{q_2''}{k})^{0.8}$$ (40)

$$A_3 = \frac{4}{(5n + 3)} \, q_2'' \, x_2.$$ (41)

For uniform fluid conditions, T_{f2} is equal to T_f^*, and the above expression reduces to the local integrated energy equation with J equal to zero.

The boundary layer integrals in the above expression are dependent on the similarity parameters n and J. Since the value of n is determined by equation (33) or (35), the only adjustable parameter is J.

Solution of the above expression for J initially looks difficult. In practice, however, solution is straightforward and, for the present investigation, has been accomplished by iterating on the form

$$\frac{\int f' \theta \, d\eta}{- \theta'_w} = \frac{A_3 - \dot{m}_2^{i-1} c_p (T_{f_2} - T_f^*)}{4 \, Pr \, q_2'' \, x_2} \tag{42}$$

where $\dot{m}_2^{i-1}$ is the value of $\dot{m}_2$ from the previous iteration. The ratio of the LHS of the equation is a strong function of J for a given value of n as depicted in Figure 3 for a Prandtl number of 0.7, and convergence of the above procedure has not been a problem.

In summary, for a specified heat flux problem, the similarity parameter n is determined directly from equation (33) or (35). For a uniform environmental fluid temperature, the similarity parameter J is equal to 0. Otherwise, the value of J is determined by iterating on equation (42). All the boundary layer parameters are uniquely determined by these values of n and J. For situations where similarity conditions are imposed, the similarity solutions are obtained. This is not the case for the method developed by Raithby, et al. (1975, 1977, 1978). For variable conditions where an exact similarity solution does not exist, the MLS method provides an estimate of "equivalent" similarity conditions including velocity and temperature profiles. This estimate is achieved by requiring conservation of energy and the same local heat flux at position x_2.

In the above development, the heat flux variation was assumed to be specified. This situation is not always the case, as the temperature distribution is sometimes given. In order to calculate the similarity parameters, energy consistency between the specified problem and the MLS method is required. The heat flux as given by equation (24) is

$$q'' = - k \, \theta'_w \, (\frac{g \, \beta}{4\nu^2})^{1/4} \, \Delta T^{5/4} \, x^{-1/4} \tag{24}$$

so the integrated heat flux for constant properties is proportional to the following integral

$$Q = \int q'' \, dx \propto \int \theta'_w \, \Delta T^{5/4} \, x^{-1/4} \, dx \tag{43}$$

and the expression for n becomes

14
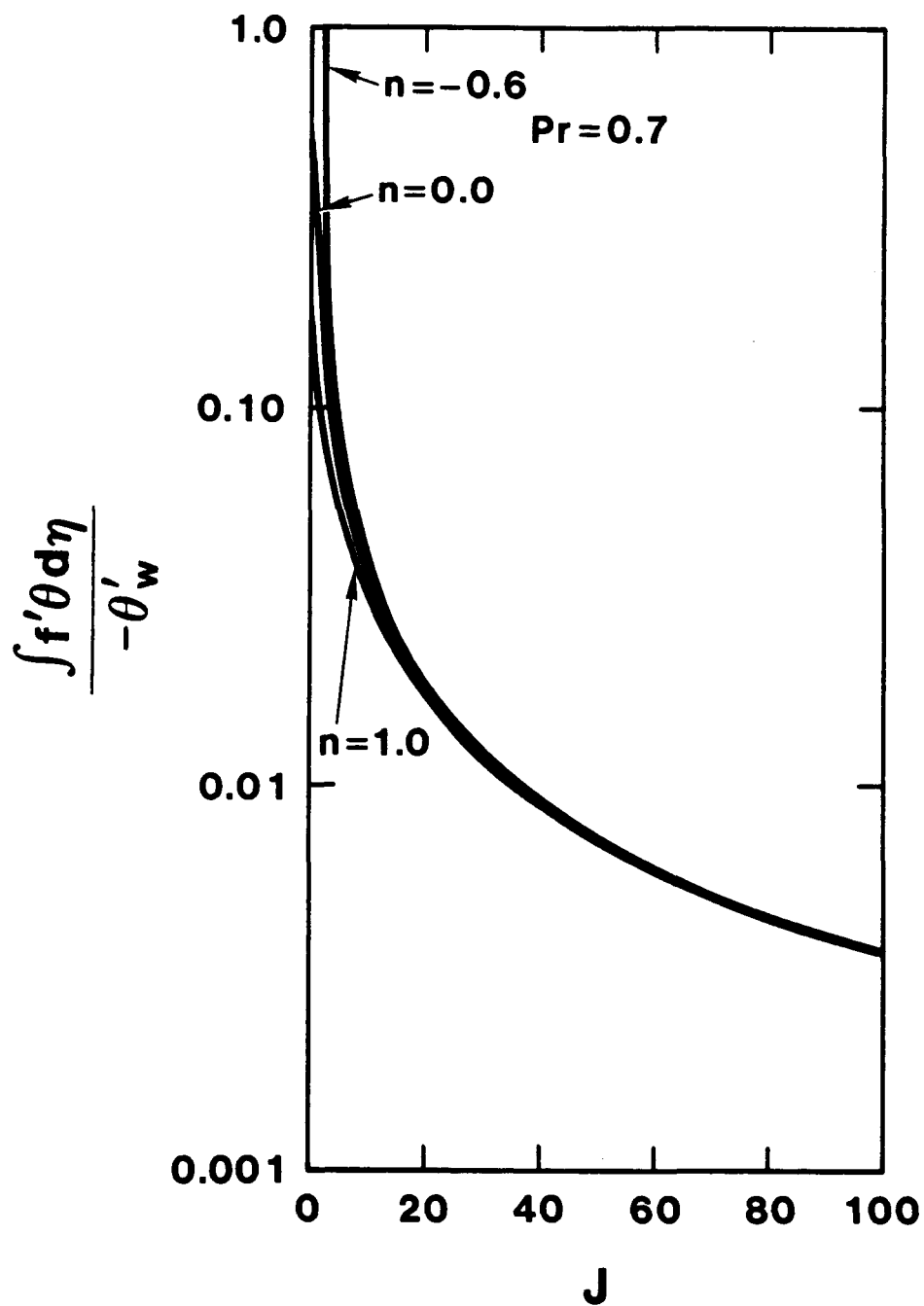
Figure 3. Variation of heat flux parameter with n and J.

$$n = \frac{1}{5} [4 \, q_2'' \, x_2 \, / \, (\dot{m}_1 \, c_p \, (\bar{T}_1 - T_f^*) + Q) - 3] \tag{44}$$

which, for x_1 and $\dot{m}_1$ equal to 0. can be written as

$$n = \frac{1}{5} \left[\frac{4 \, \theta_w' \, \Delta T_2^{5/4} \, x_2^{3/4}}{\int \theta_w' \, \Delta T^{5/4} x^{-1/4} dx} - 3 \right]. \tag{45}$$

The difficulty in evaluating the above expression is in the temperature gradient term which is a function of x. The temperature gradient for a given Prandtl number is only a function of n and J, so iteration is required on this equation and the equation given above for J.

Technically, for specified surface temperatures, the MLS method is not a local similarity approach since the answer at x depends on the results at the upstream locations. Iteration is required for the variation of the similarity parameters with x. However, this iteration is easily accomplished since the only term that depends on n and J is θ_w', and convergence is rapid for the cases analyzed in this report.

While specified temperatures are a convenient analytical case, the wall temperature and wall heat fluxes are usually coupled to each other through heat conduction, and either the wall temperature or the heat flux can be used in the solution scheme. For the present method, heat fluxes are considerably more convenient than temperatures since no iteration in the MLS method is involved.

16

2. Exponential Distribution

For the exponential distribution, the temperature difference between the wall and the fluid is given by

$$\Delta T(x) = T_w(x) - T_f(x) = M \, e^{mx}. \qquad (46)$$

For similarity, the fluid temperature variation must be of the same form, or (Jaluria (1980))

$$T_f(x) - T_r = \frac{J \, M}{4} (e^{mx} - 1) \qquad (47)$$

where the reference temperature T_r is the fluid temperature at $x = 0$. As for the power-law profile, a uniform temperature fluid results in a J value equal to 0. Note that the similarity variable m is dimensional and has units of inverse distance.

As can be seen from equation (46), the temperature difference at the leading edge can not be equal to 0. Additional problems with the exponential distribution, such as non-zero momentum and heat flow at the leading edge, are discussed by Gebhart and Mollendorf (1969). In practice, these difficulties make the exponential distribution much less useful than the power-law distribution. These problems will also be evident in the evaluation of the exponential distribution later on in this report.

The stream function and similarity variables for this case are the same as for the power-law distribution with x replaced by (1/m), or (Gebhart and Mollendorf (1969))

$$\psi = 4 \left(\frac{Gr_m}{4}\right)^{1/4} \nu \, f(\eta) \qquad (48)$$

$$\eta = \left(\frac{Gr_m}{4}\right)^{1/4} y \, m \qquad (49)$$

$$\theta(\eta) = \frac{T - T_f(x)}{T_w - T_f(x)} \qquad (50)$$

where

$$Gr_m = \frac{g \, \beta \, \left(\frac{1}{m}\right)^3 (T_w(x) - T_f(x))}{\nu^2} \qquad (51)$$

and the fluid velocity in the x direction becomes

$$u = \frac{\partial \psi}{\partial y} = \frac{\partial \psi}{\partial \eta} \frac{\partial \eta}{\partial y}$$

$$= 2 \nu \, Gr_m^{1/2} \, m \, f'. \tag{52}$$

The boundary layer partial differential equations (6)-(8) reduce to a set of coupled ordinary differential equations when the similarity variables are imposed. For the exponential distribution, the local similarity form of these equations is (Jaluria (1980))

$$f''' + f f'' - 2 f'^2 + \theta = 0 \tag{53}$$

$$\frac{\theta''}{Pr} + f \theta' - 4 f' \theta - J f' = 0 \tag{54}$$

with the appropriate boundary conditions. These equations have been solved in the present study by the finite difference method as summarized by Webb (1989).

The first term to be evaluated for substitution into the global energy equation (5) is the difference between the fluid temperature at location 2 and T_f^*. Expressing the fluid temperature difference in terms of the similarity parameter J,

$$T_{f_2} - T_f^* = \frac{J \, M}{4} (e^{mx_2} - e^{mx^*}). \tag{55}$$

M can be evaluated at location x_2, and the above equation can be rewritten as

$$T_{f_2} - T_f^* = \frac{J \, \Delta T_2}{4} (1 - e^{m(x^* - x_2)}). \tag{56}$$

Using the similarity parameters defined above along with equation (56), the global energy equation (5) becomes

$$\dot{m}_1 \, c_p \, (\bar{T}_1 - T_f^*) + \bar{q}_2'' \, \Delta x$$

$$= \dot{m}_2 \, c_p \, (\frac{J}{4} (1 - e^{m(x^* - x_2)}) + \frac{\int f' \theta \, d\eta}{\int f' \, d\eta}) \, \Delta T_2. \tag{57}$$

Expressions for the mass flow rate and the temperature difference at location 2 will now be developed. The mass flow rate per unit width can be expressed in terms of the local similarity variables as

$$\dot{m} = \rho \bar{V} A / W = \rho \bar{V} \delta$$

$$= 4 \mu \int f' d\eta \; (\frac{g \beta}{4\nu^2})^{1/4} \; (\frac{1}{m})^{3/4} \; \Delta T^{1/4}. \tag{58}$$

The heat flux relationship

$$q'' = - k \; \theta'_w \; (\frac{g \beta}{4\nu^2})^{1/4} \; \Delta T^{5/4} \; (\frac{1}{m})^{-1/4} \tag{59}$$

can be used to get the temperature difference as a function of (1/m), or

$$\Delta T^{5/4} = (\frac{q''}{- k \; \theta'_w}) \; (\frac{g \beta}{4\nu^2})^{-1/4} \; (\frac{1}{m})^{1/4} \tag{60}$$

Note that for a similarity solution, the temperature gradient at the wall and m are both constant, and the heat flux variation can be written as

$$q'' \; \alpha \; \Delta T^{5/4} \; \alpha \; e^{5mx/4}. \tag{61}$$

Using equation (60), the mass flow rate equation can be rewritten as

$$\dot{m} = 4 \mu \int f' d\eta \; (\frac{g \beta}{4\nu^2})^{0.2} \; (\frac{1}{m})^{0.8} \; (\frac{q''}{- k \; \theta'_w})^{0.2} \tag{62}$$

and the global energy equation (57) then becomes

$$\dot{m}_1 c_p \; (\bar{T}_1 - T_f^*) \; + \; \bar{q}_2'' \; \Delta x$$

$$= 4 \; Pr \int f' d\eta \; (\frac{q_2''}{- \theta'_w})$$

$$(\frac{J}{4} \; (1 - e^{m(x^* - x_2)}) + \frac{\int f' \theta \, d\eta}{\int f' d\eta}) \; \frac{1}{m}. \tag{63}$$

The same similarity variables can be used in the integrated local boundary layer equations (9) and (10) resulting in the following equations for the boundary layer quantities

Momentum

$$3 \int f'^2 \, d\eta = \int \theta \, d\eta - f''_w \tag{64}$$

Energy

$$5 \int f' \theta \, d\eta = - \frac{\theta'_w}{Pr} - J \int f' \, d\eta \tag{65}$$

where the parameter m does not appear.

These relationships are a measure of the shape of the velocity and temperature boundary layer profiles and are useful for checking the accuracy of the numerical solution of the local similarity equations. They are also helpful if numerical fits are generated to some of the boundary layer integrals as these expressions can be used to ensure consistency among the various parameters.

Rearranging the local boundary layer energy equation (65) and substituting it into the global energy equation (63) results in

$$(\dot{m}_1 \, c_p \, (\bar{T}_1 - T_f^*) + \bar{q}''_2 \, \Delta x) \, / \, q''_2$$

$$= - \frac{\frac{J}{m} (1 - e^{m(x^* - x_2)}) + \frac{4}{m} \int f' \theta \, d\eta \, / \int f' \, d\eta}{J + 5 \int f' \theta \, d\eta \, / \int f' \, d\eta}. \tag{66}$$

The ratio of the first terms in the numerator and denominator on the RHS and of the second terms on the RHS must both be equal to the LHS. For the second terms,

$$\frac{4}{5m} = [(\dot{m}_1 \, c_p \, (\bar{T}_1 - T_f^*) + \bar{q}''_2 \, \Delta x) \, / \, q''_2] \tag{67}$$

or,

$$m = \frac{4}{5} [q''_2 \, / \, (\dot{m}_1 \, c_p \, (\bar{T}_1 - T_f^*) + \bar{q}''_2 \, \Delta x)]. \tag{68}$$

Similarly, making use of equation (67), the first terms give

$$x^* = x_2 - 1.609 \, / \, m. \tag{69}$$

If x_1 is taken to be at the leading edge of the plate ($x_1=0$.) with no initial mass flow rate, then $\Delta x = x_2$, and the above equation for mx_2 simplifies considerably to

$$mx_2 = \frac{4}{5} \frac{q_2''}{\bar{q}_2''}.$$ (70)

The value of the similarity parameter m is just a function of the ratio of the local to the average heat flux up to that point and x_2. The fluid temperature evaluated at x^* is that required for global energy conservation.

Surprisingly, the stratification parameter, J, is independent of global conservation of energy. Instead, the value of J is determined by the local value of the heat flux, q_2''. Equating the conservation of energy equations (2) and (68) gives

$$\dot{m}_2 \, c_p \, (\bar{T}_2 - T_f^*) = \frac{4}{5m} \, q_2''$$ (71)

where the values on the RHS are known. Expanding the LHS of the above equation results in the expression

$$\dot{m}_2 \, c_p \, \left(\frac{\int f'\theta \, d\eta}{\int f' \, d\eta} \Delta T_2 + T_{f_2} - T_f^* \right) = \frac{4}{5m} \, q_2''.$$ (72)

This equation includes the effect of temperature stratification on the local energy balance. This equation is of the same form as equation (38) derived for the power-law distribution. The same techniques outlined for the solution of equation (38) have been used for equation (72) above.

In summary, for a specified heat flux problem, the similarity parameter m is determined directly from equation (70) or (72). For a uniform environmental fluid temperature, the similarity parameter J is equal to 0. Otherwise, the value of J is determined by iterating on equation (72). All the boundary layer parameters are uniquely determined by these values of m and J. For situations where similarity conditions are imposed, the similarity solutions are obtained. This is not the case for the method developed by Raithby, et al. (1975, 1977, 1978). For variable conditions where an exact similarity solution does not exist, the MLS method provides an estimate of "equivalent" similarity conditions including velocity and temperature profiles. This estimate is achieved by requiring conservation of energy and the same local heat flux at position x_2.

21

In the above development, the heat flux variation was assumed to be specified. This situation is not always the case, as the temperature difference is sometimes given. In order to calculate the similarity exponent on the temperature distribution, energy consistency between the specified problem and the MLS method is required. The heat flux as given by equation (59) is

$$q'' = - k \; \theta'_w \; (\frac{g \; \beta}{4 \nu^2})^{1/4} \; \Delta T^{5/4} \; m^{1/4} \tag{59}$$

so the integrated heat flux for constant properties is proportional to the following integral

$$Q = \int q'' \; dx \propto \int \theta'_w \; \Delta T^{5/4} \; m^{1/4} \; dx \tag{73}$$

and the expression for m becomes

$$m = \frac{4}{5} \; [q''_2 \; x_2 \; / \; (\dot{m}_1 \; c_p \; (\bar{T}_1 - T^*_f) + Q)] \tag{74}$$

which, for x_1 and $\dot{m}_1$ equal to 0. can be written as

$$m = \frac{4}{5} \; (\frac{\theta'_w \; \Delta T^{5/4}_2 \; m^{1/4} \; x_2}{\int \theta'_w \; \Delta T^{5/4} \; m^{1/4} \; dx}) . \tag{75}$$

The difficulty in evaluating the above expression is that m is a function of x, so iteration is required on this one equation. Note that θ'_w is not a function of m or x but is simply a function of J and the Prandtl number.

Technically, for specified surface temperatures, the MLS method is not a local similarity approach since the answer at x depends on the results at the upstream locations. Iteration is required for the variation of the similarity parameters with x. However, this iteration is easily accomplished since the only term that depends on m is m itself, and convergence is rapid for the cases analyzed in this report.

While specified temperatures are a convenient analytical case, the wall temperature and wall heat fluxes are usually coupled to each other through heat conduction, and either the wall temperature or the heat flux can be used in the solution scheme. For the present method, heat fluxes are considerably more convenient than temperatures since no iteration in the MLS method is involved.

III. Evaluation

The Modified Local Similarity (MLS) method derived above has been applied to a number of nonsimilar wall temperature and heat flux cases with uniform fluid temperature and to an isothermal plate in a stratified fluid environment. In each case, the power-law and exponential distributions have been evaluated. Variation of the similarity variables and of the predicted surface behavior is presented.

The results in this section compare the predictions from the MLS method with those from other approaches and, for the case of an isothermal plate in a stratified fluid, to experimental data. The results from another possible implementation of the local similarity approach in addition to the MLS method are also given. While the MLS method is based on conservation of energy as the boundary layer develops and matching the local heat flux, another reasonable approach would be matching the local value of the specified parameter (temperature difference or heat flux) as well as the local slope of that parameter.

For example, consider the power-law distribution as applied to an exponential variation of the temperature difference. Equating the local temperature difference as well as the slope of the temperature difference at any point x with the similarity distribution,

$$\Delta T = e^x = N x^n \tag{76}$$

$$d(\Delta T)/dx = e^x = N n x^{n-1} \tag{77}$$

results in the requirement that

$$n = x. \tag{78}$$

As another example, consider the power-law distribution for an exponential variation of the heat flux. Equating the local value and the slope

$$q''/k = e^x = A x^{(5n - 1)/4} \tag{79}$$

$$d(q''/k)/dx = e^x = \frac{5n - 1}{4} A x^{5(n - 1)/4} \tag{80}$$

gives the result that

$$n = 0.8x + 0.2. \tag{81}$$

The predictions from this application of the local similarity approach will be presented in the results that follow and will be referred to as the LS* method.

A. Uniform Fluid Temperature

For uniform fluid temperature conditions, the MLS and LS* methods have been applied to specified wall temperature and specified heat flux cases. Results to these cases for a number of other methods are summarized by Yang, et al. (1982) for a Prandtl number of 0.7 where the property term is assumed equal to 1.0, or

$$\left(\frac{g\,\beta}{4\nu^2}\right) = 1.0. \tag{82}$$

In all these cases, the stratification parameter, J, is equal to 0. since the fluid temperature is uniform. The power-law and exponential distributions will be discussed for each case.

The results presented by Yang, et al. (1982) are in terms of transformed surface conditions as given by Kao, et al. (1977); these transformations are summarized in the appendix. The use of these transformed variables can distort the surface condition variation, and this method of presentation will not be used. The results that are given in this section are in terms of physical variables, i.e., the variation of the temperature difference or the temperature gradient at the surface, not the variation of the transformed variable.

The results from the MLS method and the LS* approach will be compared to the following predictions. Note that the MLS and LS* methods solve two coupled ODE's.

1. Numerical - as given by Kao, et al. (1977).
2. Kao LS - Kao, et al. (1977) presents local similarity results in terms of his transformed coordinates. This approach solves two coupled ODE's similar to the MLS and LS* methods. The equations are given in the appendix.
3. Kao method - The method developed by Kao, et al. (1977) uses transformed coordinates and is basically a perturbation approach. Four coupled ODE's are solved in this approach.
4. Yang method - Yang, et al. (1982) uses the transformed coordinates developed by Kao with a series expansion of the similarity parameters. Six coupled ODE's are solved in this method.

The Kao and Yang methods are more complicated than the MLS method or Kao LS approach since more ODEs are involved. In addition to the above results, predictions from other methods, such as the integral approach, will be included where available.

1. Specified Surface Temperature

Since the surface temperature is known, the comparisons are based on the temperature gradient at the surface which is related to the local heat transfer coefficient. The values of the similarity parameters are used to compare the MLS and LS* temperature variation with the desired behavior.

a. $\Delta T = e^x$

<u>Power-Law Distribution</u> The variation of the similarity variable n with x is shown in Figure 4a for the MLS and LS* approaches. In both cases, the value of n increases considerably with increasing x. Figure 4b shows the desired temperature difference as well as the variation predicted by both approaches. The predictions from the methods depend on n which itself is a function of x as given in Figure 4a. Therefore, in Figure 4b, two curves corresponding to the two x values of 0.5 and 2.0 are shown for each approach. In general, the variation of the temperature difference is reasonably close to the desired behavior. The temperature difference variation is well represented by the power-law distribution in both methods.

The surface temperature gradient as a function of x is depicted in Figure 5. The gradient is underpredicted by the MLS method by approximately 5%. While the error is larger than the other methods, the magnitude is still relatively small. For the LS* approach, a slight overprediction of the gradient, especially near the front of the plate, is noted. This behavior is also seen for the Kao LS method. Predictions for the Kao and Yang methods are not shown in this figure since both approaches yield predictions indistinguishable from the numerical results.

<u>Exponential Distribution</u> For the exponential distribution, the MLS and LS* approaches yield the similarity solution with m equal to 1.0. Even with this ideal comparison case, the wall temperature gradient shown in Figure 6 is overpredicted, especially at small x values. The reason for this difference is the non-zero momentum and heat flow at the leading edge as alluded to earlier. According to Gebhart and Mollendorf (1969), the exponential distribution results are reasonable only if mx is much greater than 1.0. The results given in Figure 6 are consistent with this criteria.

b. $\Delta T = \sin x$

<u>Power-Law Distribution</u> Figure 7a shows the behavior of the similarity variable n with x. For the MLS method, n decreases with distance up the plate and changes sign at an x of about 2.15. For the LS* approach, n also decreases with distance up the plate and changes sign at an x value of $\pi/2$. The temperature difference is given in Figure 7b for x of 1.0 and 2.5. For small x values ($< \sim\pi/2$), both methods give a good approximation of the sinusoidal temperature difference. For larger x values, the MLS distribution becomes increasingly poor, especially when n becomes negative.
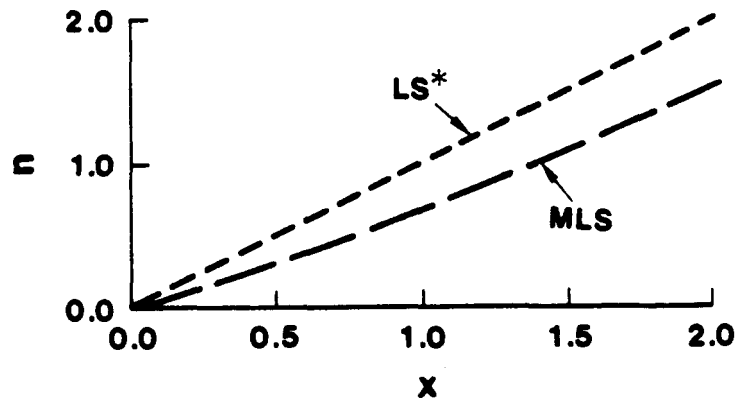
Figure 4a.   Variation of n for $\Delta T = e^x$.
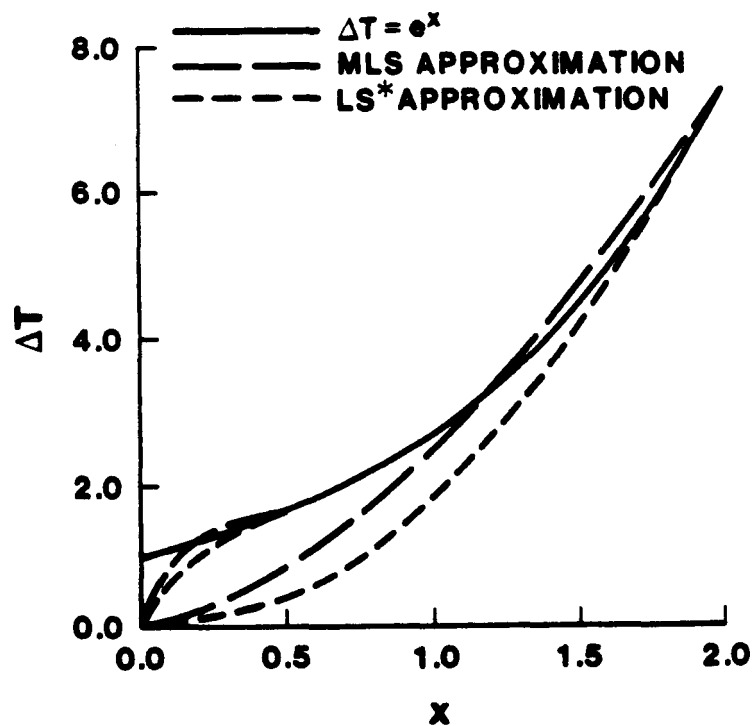   PL Distribution.

Figure 4b.   Approximation of ΔT for $\Delta T = e^x$.
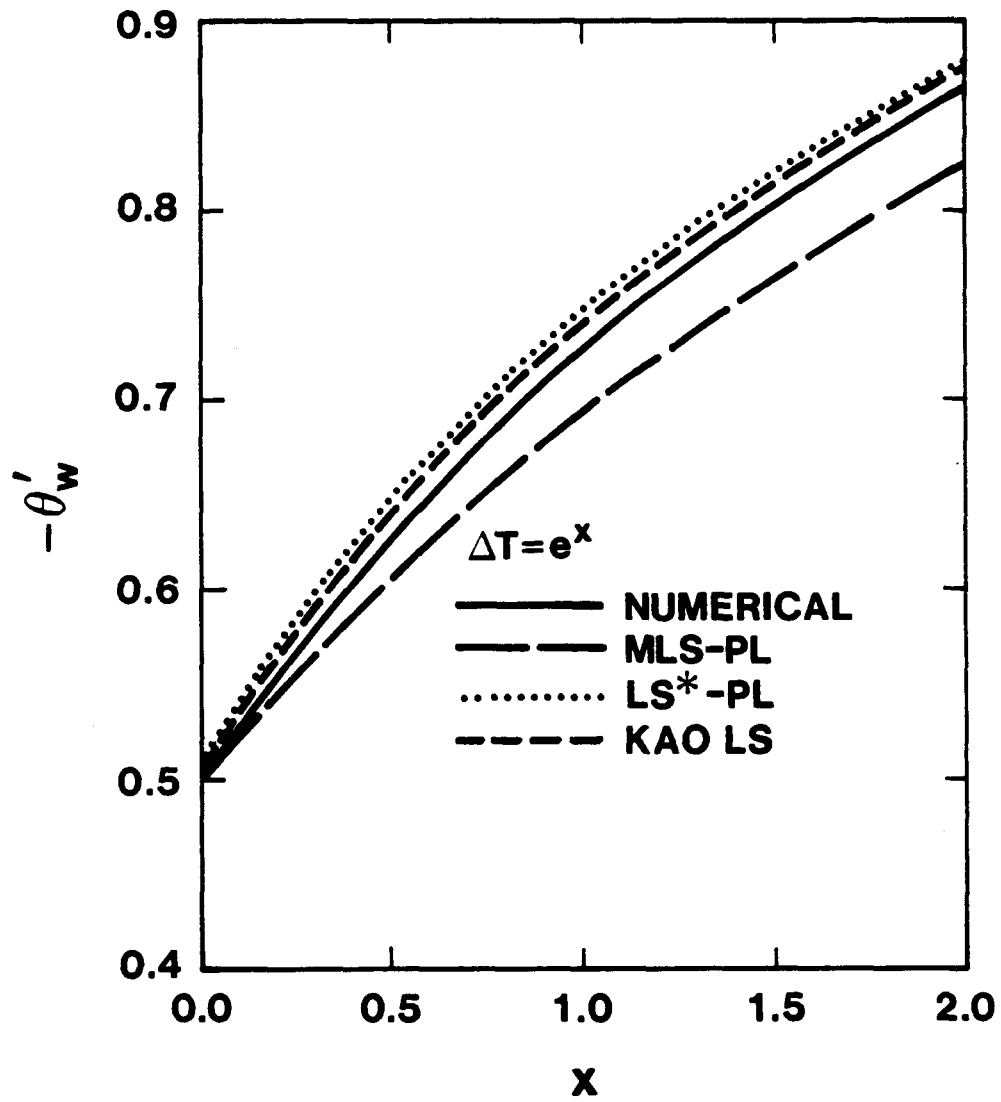   PL Distribution.

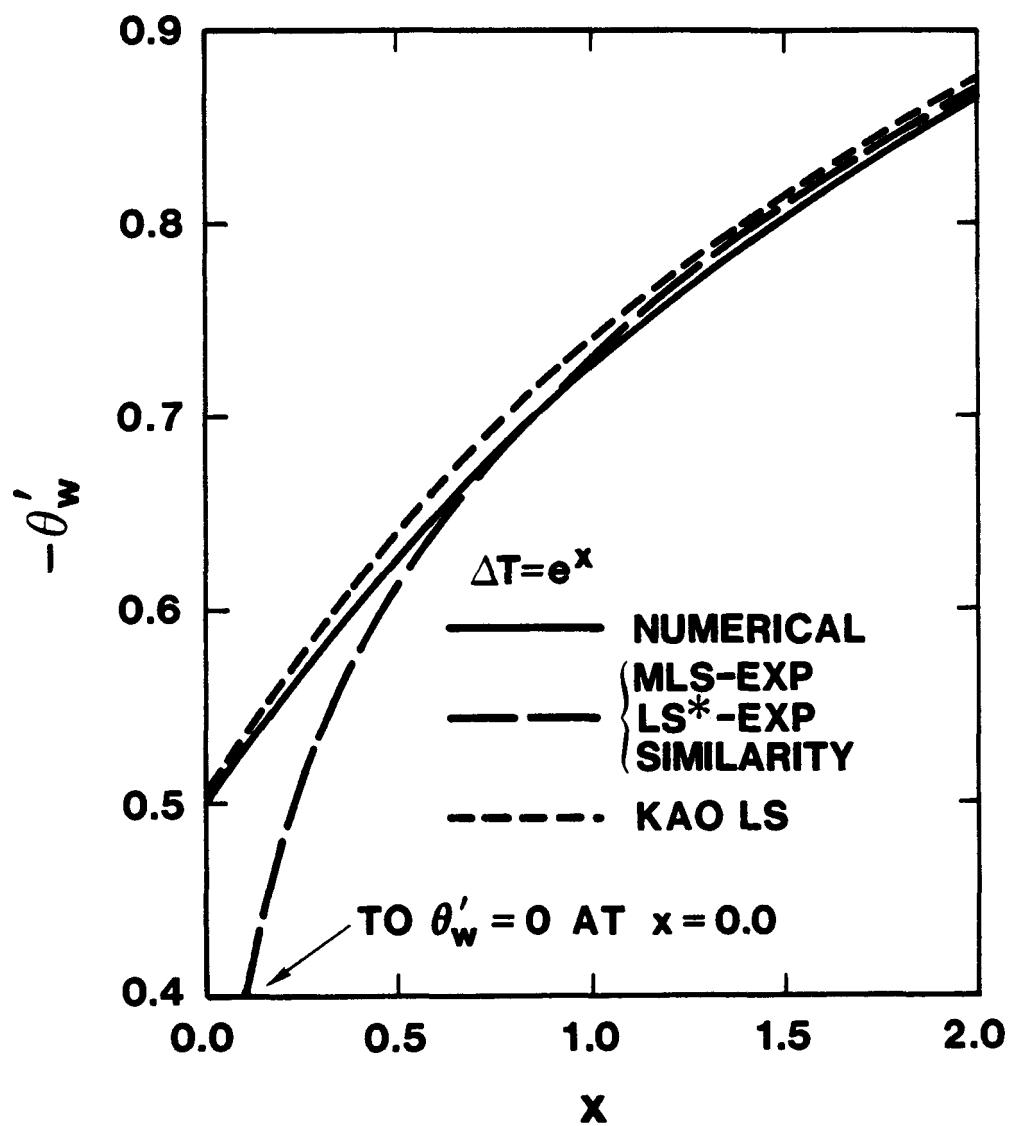Figure 5. Surface temperature gradient for $\Delta T = e^x$. PL Distribution.

27

Figure 6.   Surface temperature gradient for $\Delta T = e^x$.
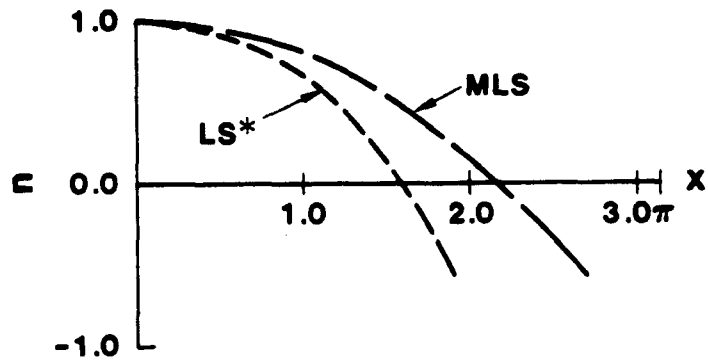Exp Distribution.

Figure 7a.   Variation of n for ΔT - sin x.
            PL Distribution.
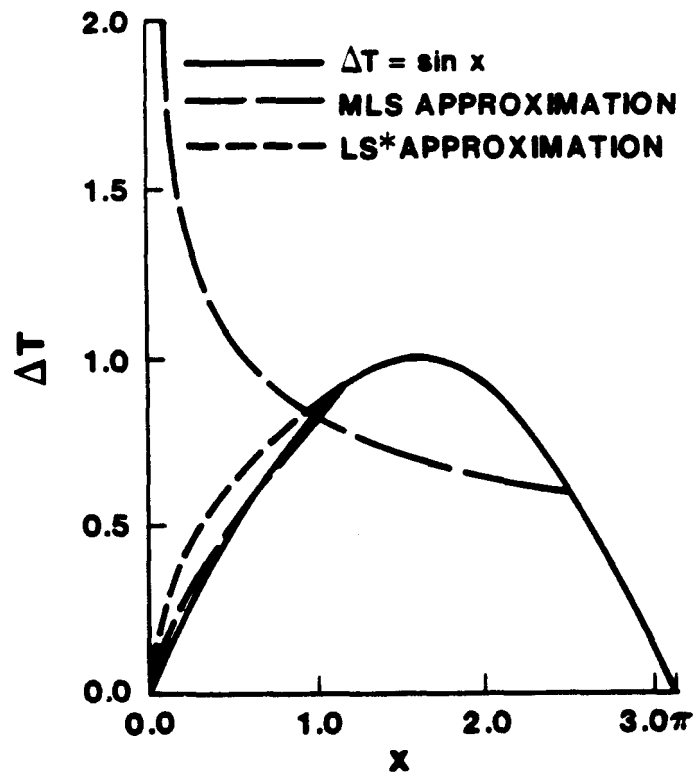

Figure 7b.   Approximation of ΔT for ΔT - sin x.
            PL Distribution.

The surface temperature gradient as a function of x is depicted in Figure 8 for a number of other methods. The Yang method gives excellent results up to an x value of 2.2 after which the method is no longer applicable due to convergence problems. The Kao method also gives good results out to an x value of 2.3; after this point, the Kao method no longer converges. The Kao local nonsimilarity (LNS) results are surprisingly poor; only results out to an x value of 2.0 are given by Kao (1976). Finally, the Kao LS results show reasonable agreement for the entire problem, although a systematic underprediction is evident.

Results for the MLS and LS* power-law approaches are shown in Figure 9. For small x values, the gradient is well predicted. For large x values, the MLS method overpredicts the temperature gradient and the location of zero heat flux, while the LS* approach underpredicts the results. While not as good as some of the other methods, the MLS approach is better than the LS* method and about the same as the Kao LS approach. This discrepancy is not unexpected due to the poor approximation of the temperature difference behavior by the MLS method at large x values.

<u>Exponential Distribution</u> For an exponential distribution, the variation of mx with x is shown in Figure 10a. The value of mx goes to 0. at x values of π and $\pi/2$ for the MLS and LS* approaches, respectively. The temperature difference comparison is given in Figure 10b. The exponential distribution has a very difficult time matching the required temperature difference variation except for small x values. Note that the value of m cannot be negative or zero, so the temperature difference must always increase with x. This situation leads to reasonable temperature variations for small x values, but very poor distributions for larger x values. For the MLS method, the value of mx is less than or equal to 1.0 for x values greater than about 1.7; for the LS* approximation, mx is always less than 1.0. Therefore, the results from the exponential distribution are expected to be poor due to the small mx values.

The results for the temperature gradient variation are shown in Figure 11. The MLS approach significantly overpredicts the wall temperature gradient, while the LS* method does just the opposite. Both methods give poor results as anticipated.
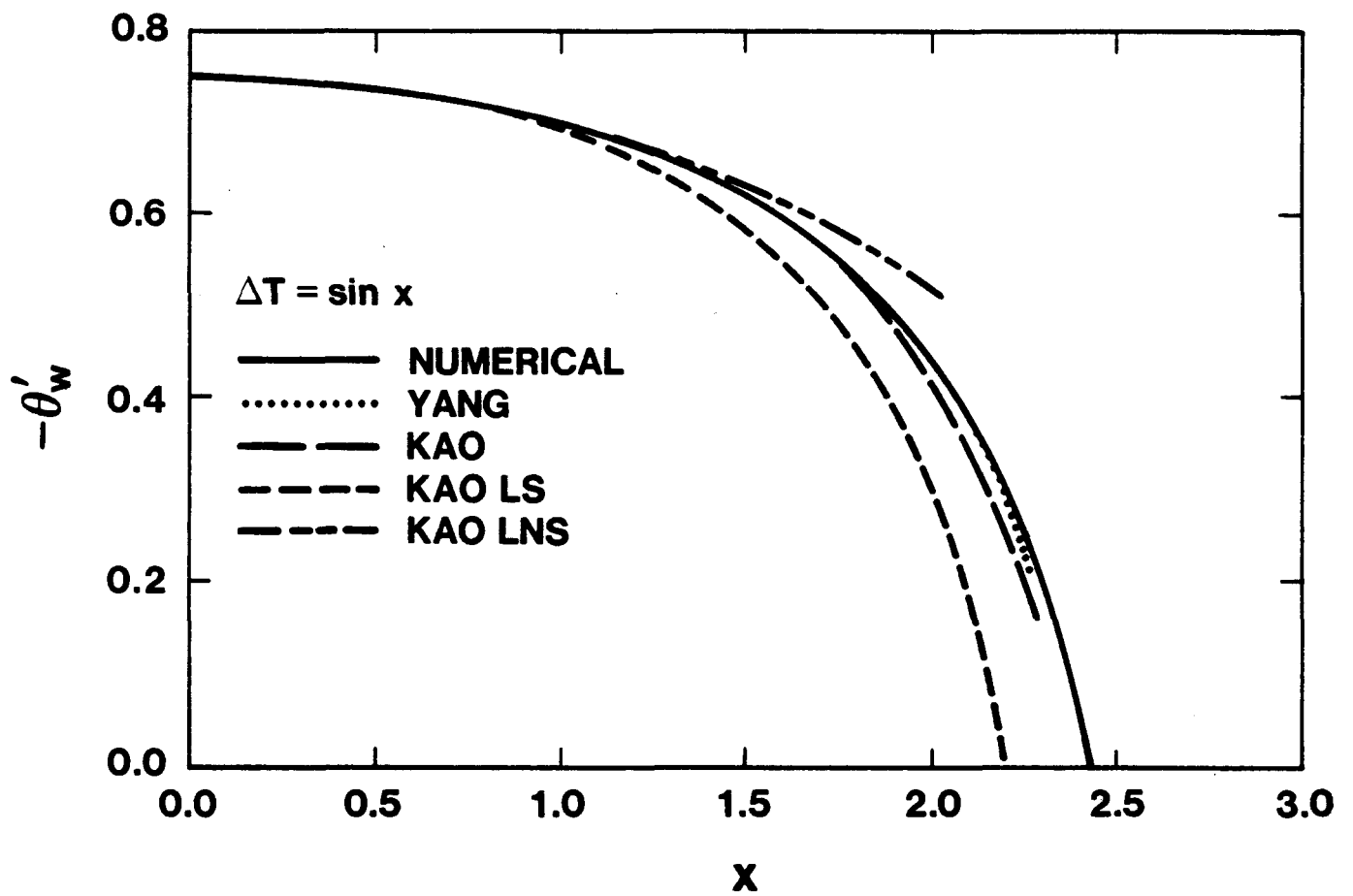
Figure 8. Surface temperature gradient for $\Delta T = \sin x$.
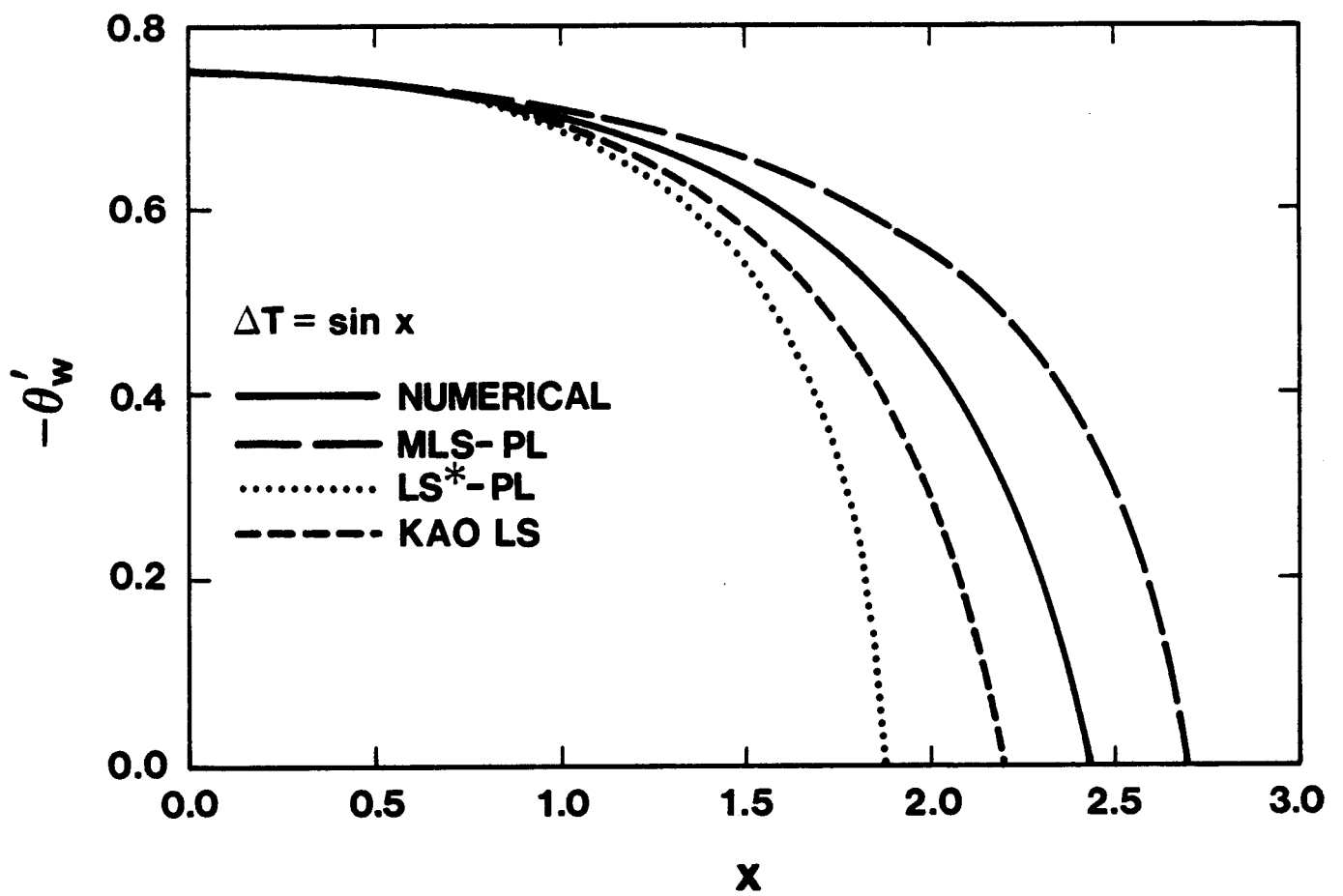Results from other methods.

Figure 9. Surface temperature gradient for ΔT = sin x.
PL distribution.

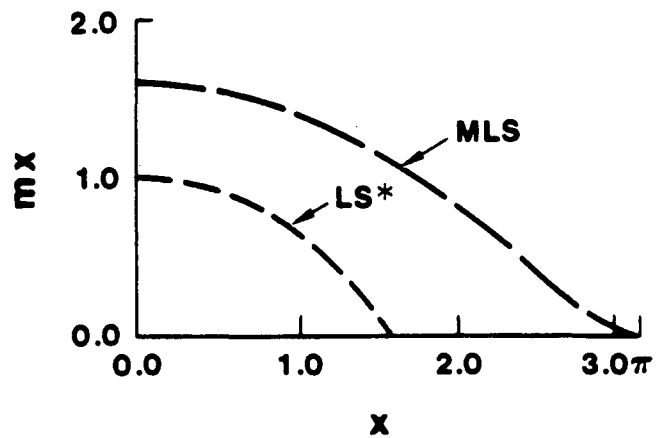Figure 10a.   Variation of mx for ΔT − sin x.
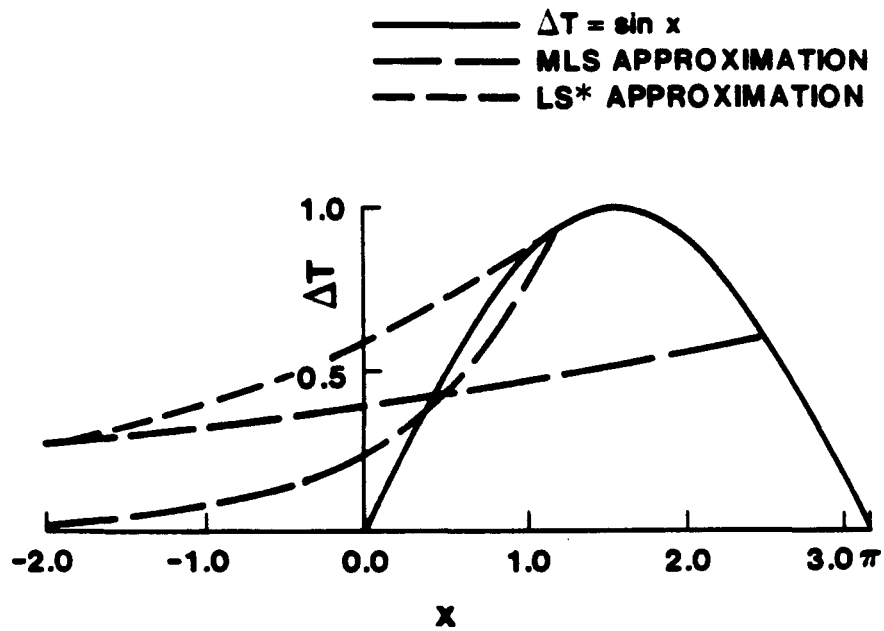   Exp distribution.

Figure 10b.   Approximation of ΔT for ΔT − sin x.
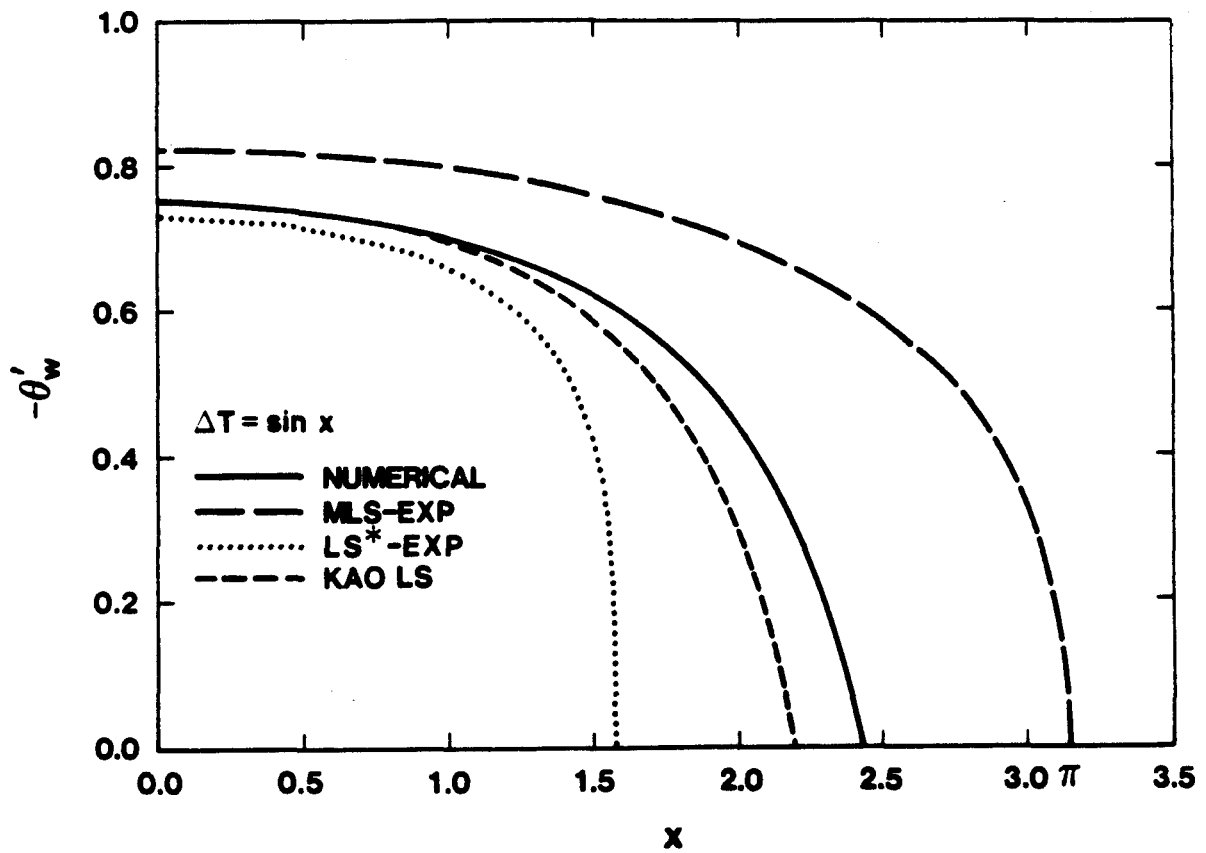   Exp distribution.

33

Figure 11.   Surface temperature gradient for $\Delta T = \sin x$.
Exp distribution.

2. Specified Wall Heat Flux

Since the surface heat flux is specified, the comparisons between the various methods are based on the wall to fluid temperature difference. The values of the similarity parameters are used to compare the MLS and LS* similarity heat flux variation with the desired behavior.

a. $q''/k = e^x$

Power-Law Distribution   Figure 12a shows the variation of the similarity variable n with x for the MLS and LS* methods which shows that n increases considerably as one goes up the plate. The rate of increase is higher for the LS* approach than for the MLS method. The heat flux distribution is given in Figure 12b for x values of 0.5 and 2.0. In general, for both cases, the heat flux variation is well represented by the power-law distribution in both methods. These conclusions are similar to those for the exponential temperature difference case discussed earlier.

The surface temperature as a function of x is depicted in Figure 13. The MLS and LS* methods both successfully predict the surface temperature variation with x. The predictions of the Kao and the Yang methods are not shown since they are indistinguishable from the numerical results. All the methods perform well for this case.

Exponential Distribution   Figure 14a depicts the variation in the similarity variable mx with x. In the MLS method, the value of mx slowly increases with x. The LS* approach reduces to the similarity results since m is a constant equal to 0.8; this result is not obvious from Figure 14a since mx is not constant. The heat flux variation for these approaches is compared to the desired variation in Figure 14b for x values of 0.5 and 2.0. The exponential distribution is an excellent approximation to the desired behavior.

The surface temperature behavior, which is given in Figure 15, is well predicted by the exponential distribution except near the leading edge. This behavior coincides well with values of mx greater than 1.0 as discussed earlier.

b. $q''/k = 1 + x$

Power-Law Distribution   Figure 16a shows the variation of n with x for both the MLS and LS* methods. The value of n increases with x in both cases. Figure 16b compares the heat flux variation for the power-law distribution to the desired variation for x values of 0.5 and 3.0. As with a number of the previous cases, the heat flux behavior is reasonably well represented by the power-law distribution in both cases.
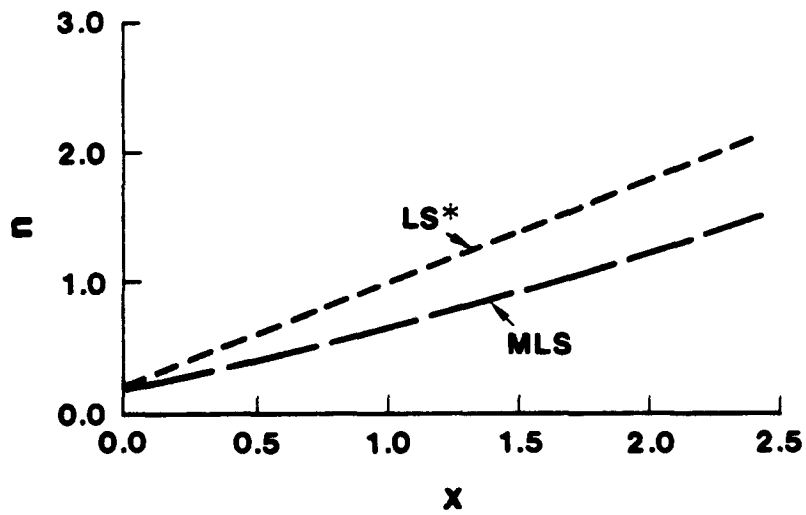
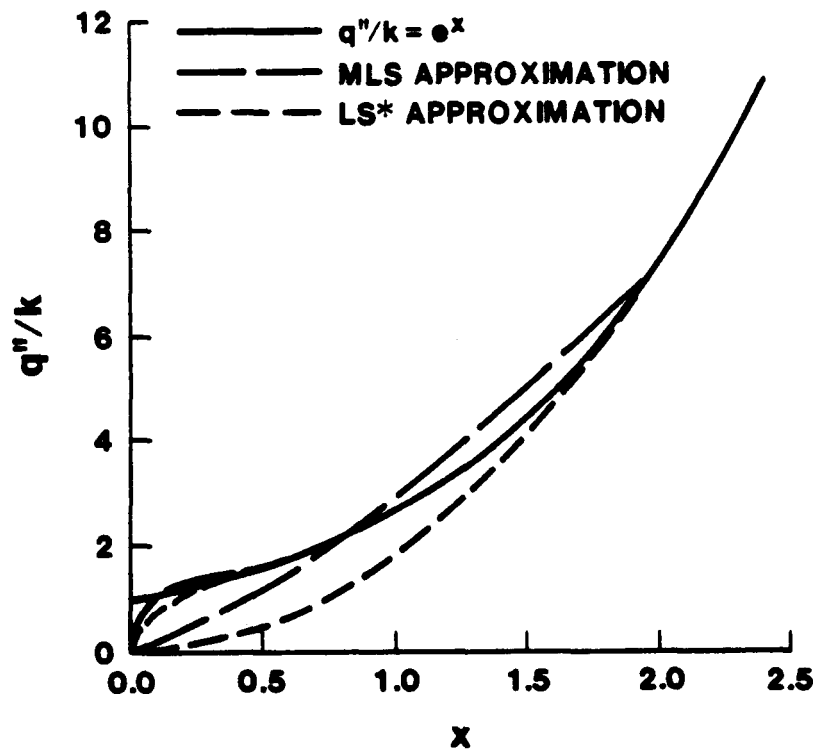Figure 12a. Variation of n for $q''/k = e^x$.
PL distribution.

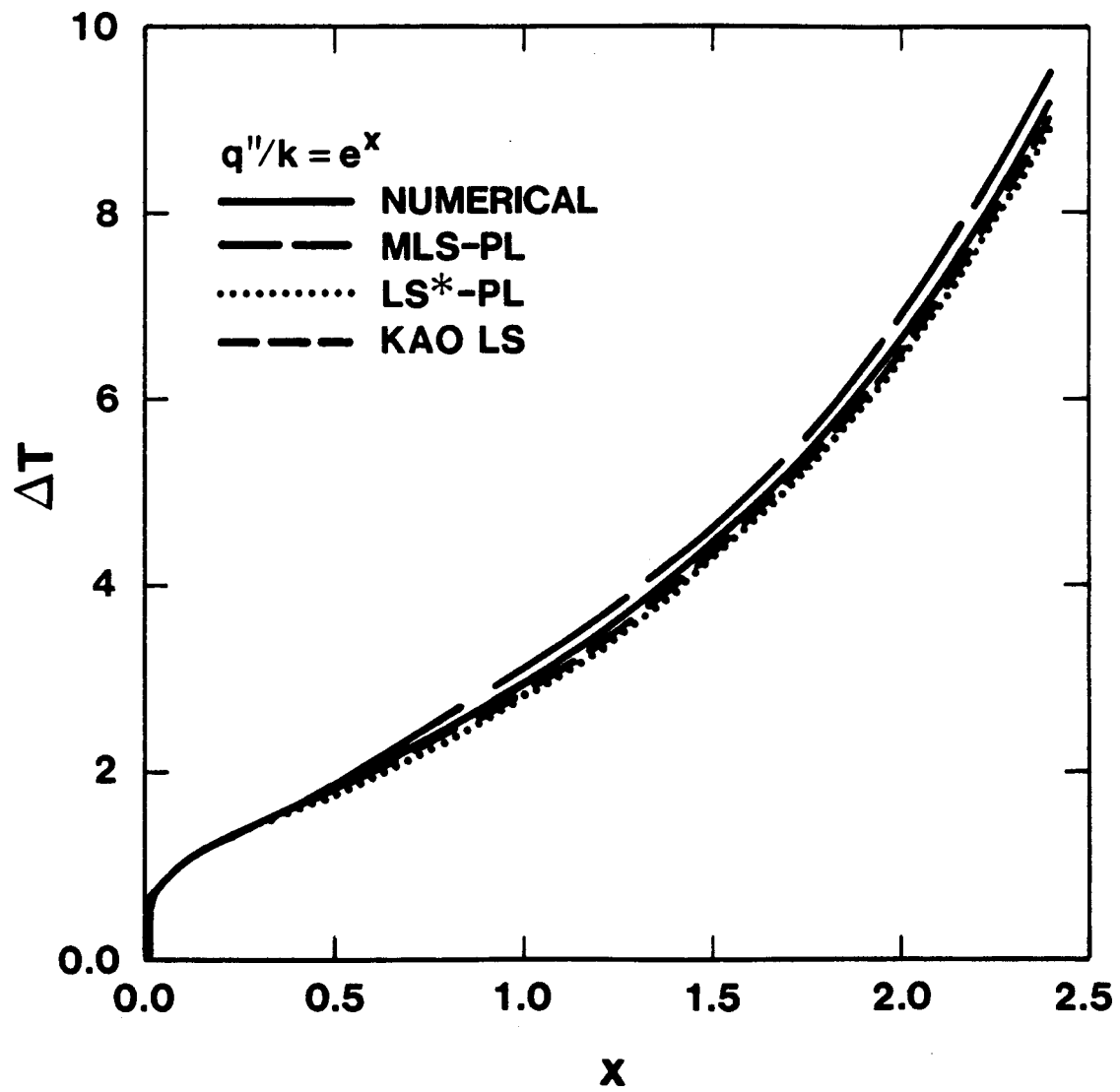Figure 12b. Approximation of $q''/k = e^x$.
PL distribution.

Figure 13.   Temperature difference for q"/k = e^x.
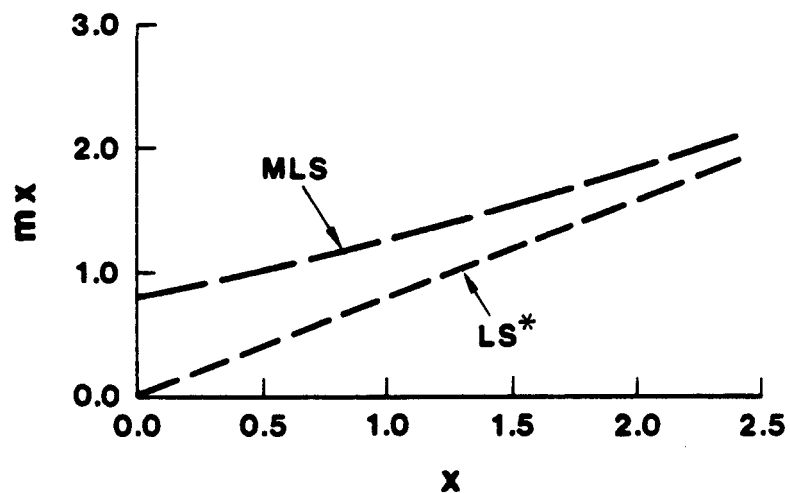   PL distribution.

37

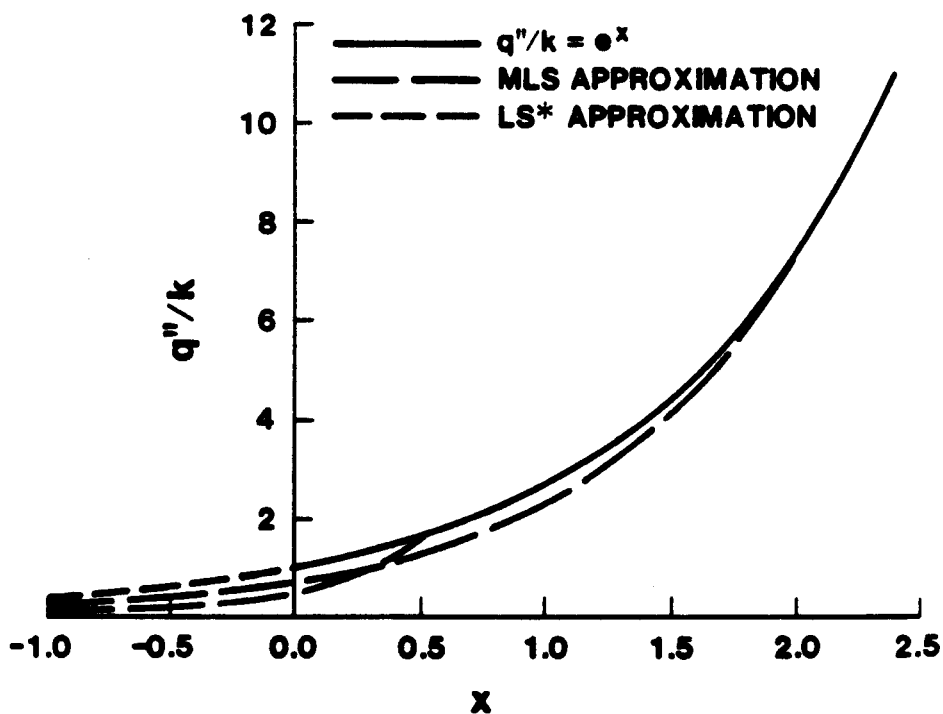Figure 14a. Variation of mx for $q''/k = e^x$.
Exp distribution.

Figure 14b. Approximation of q''/k for $q''/k = e^x$.
Exp distribution.
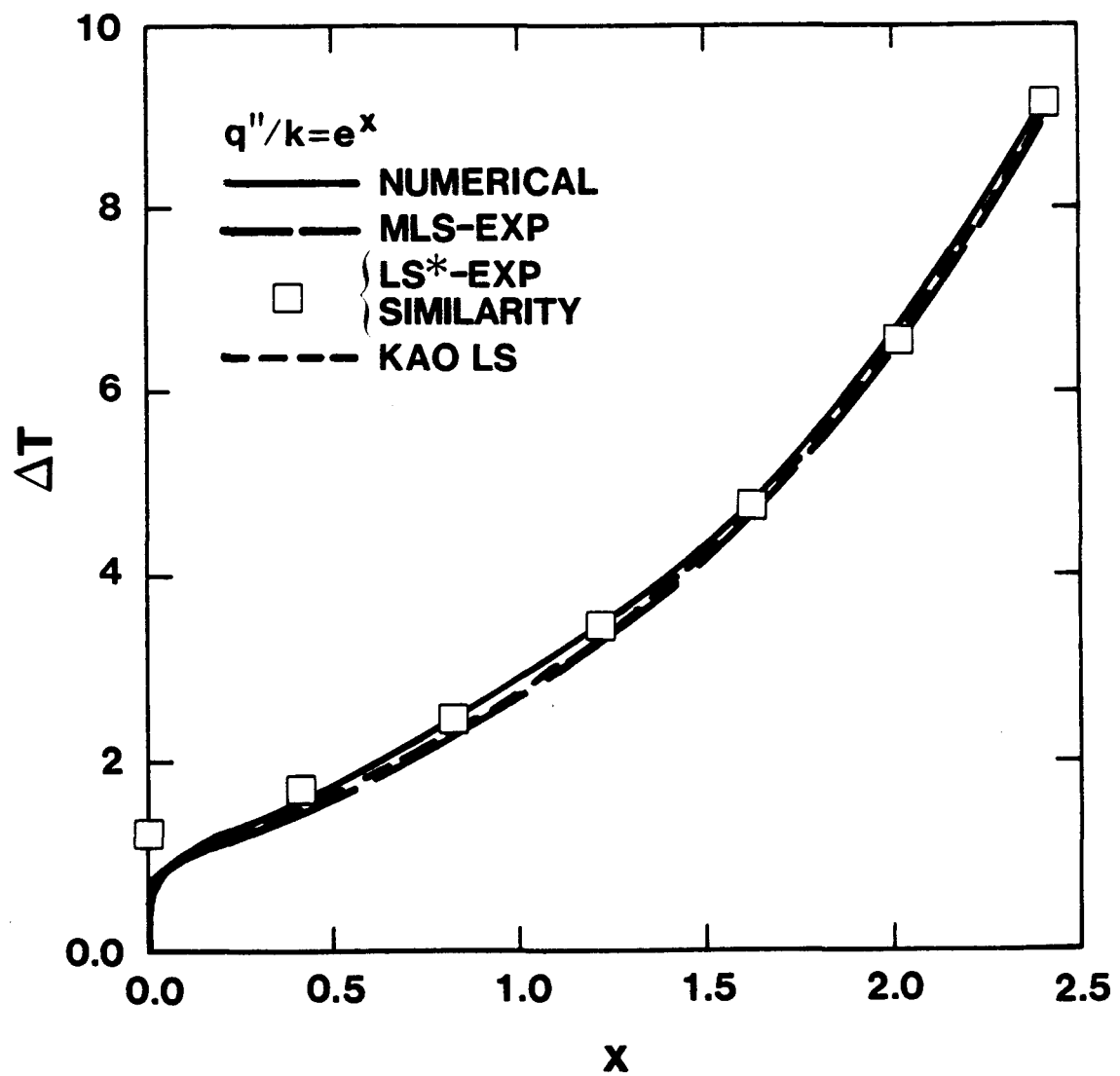
38

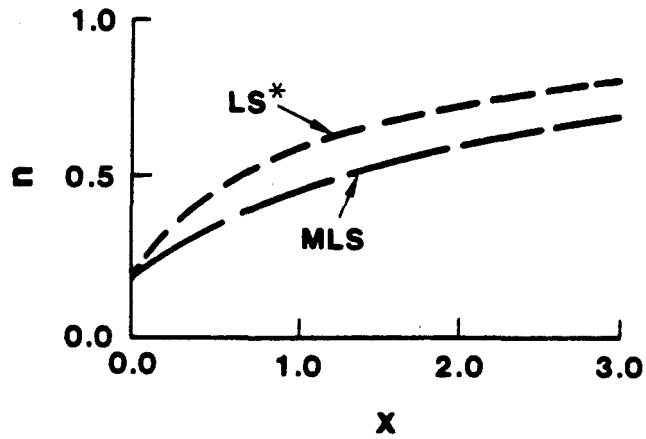Figure 15.   Temperature difference for q″/k = e^x.
Exp distribution.

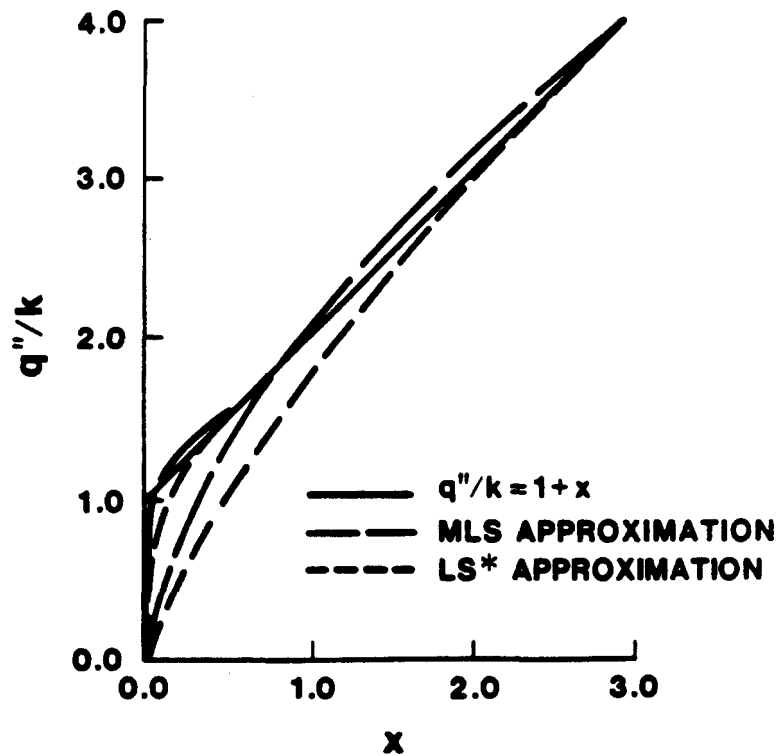Figure 16a. Variation of n for q″/k = 1 + x.
PL distribution.

Figure 16b. Approximation of q″/k for q″/k = 1 + x.
PL distribution.

40

Figure 17 shows the temperature difference variation along the plate. The answers from the Kao method and the Yang method are not given since they essentially coincide with the numerical results. The results from the integral analysis as given by Sparrow (1955) are also shown. All methods give good predictions for this case including the integral method.

Exponential Distribution The variation of mx with x is depicted in Figure 18a. The value of mx increases slowly for both the MLS and LS* approaches. However, for the LS* approach, the value of mx will never exceed 1.0 no matter how long the plate. Figure 18b shows the heat flux profiles for x values of 0.5 and 3.0. Neither method does a good job of matching the heat flux variation with the exponential distribution.

Figure 19 shows the temperature difference predictions for this case. Neither method does a very good job of predicting the temperature difference, especially compared to the other methods. This trend is expected due to the poor representation of the heat flux variation given earlier.

c. $q''/k = 1 - x$

Power-Law Distribution Figure 20a shows the variation of n with x for both the MLS and LS* methods. For the MLS approach, the value of n decreases slightly with x. The value of n in the LS* approximation decreases much faster than for the MLS approach. The heat flux variation is given in Figure 20b. The behavior of both methods is not unreasonable, although significant differences can be seen between the approximation and the desired variation.

Figure 21 gives the temperature difference variation along the plate for a number of different methods. The Kao and Yang methods diverge from the numerical solution at x values of 0.6. The Kao LS method gives widely different results. The integral results from Sparrow (1955) seem to be the best behaved, although the results could only be provided out to an x value of 0.5 due to the limited results presented by Sparrow. Figure 22 gives the MLS and LS* predictions. The MLS method provides a reasonable prediction for the surface temperature behavior; the results are superior to all the other methods based on the numerical predictions. Note that the MLS calculations have been performed out to an x value of 1.0 with no problems. The LS* predictions tend to blow up like the Kao LS results.

Exponential Distribution The variation of mx with x is depicted in Figure 23a. The value of mx decreases slowly for both the MLS and LS* approaches and is always less than 1.0. The heat flux profiles are given in Figure 23b. The MLS approximation is unreasonable for this case. The LS* heat flux variation is much closer, although this method has other problems for this case.

41
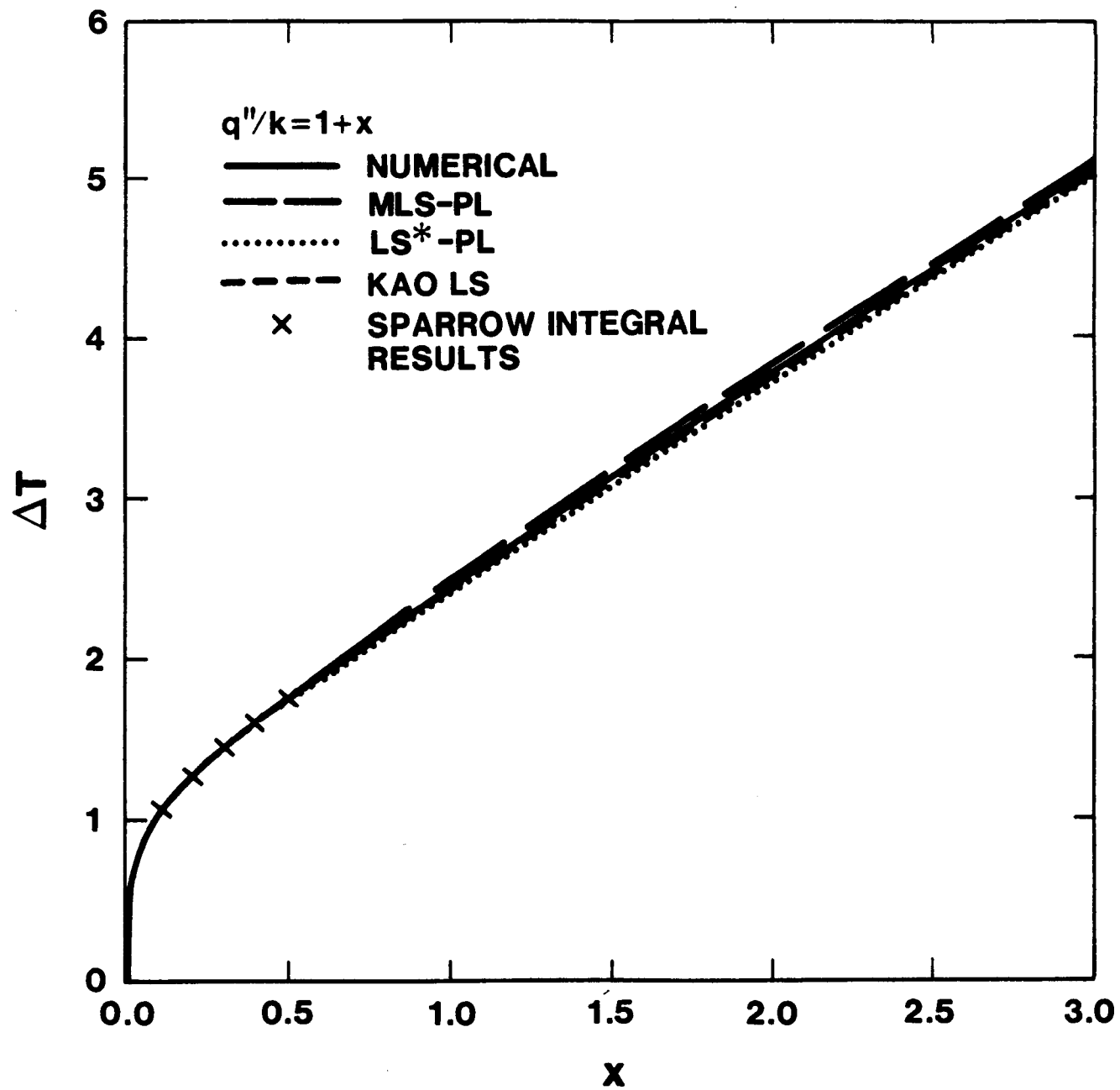
Figure 17.   Temperature difference for q"/k - 1 + x.
PL distribution.

Figure 18a.   Variation of mx for q"/k – 1 + x.
              Exp distribution.

Figure 18b.   Approximation of q"/k for q"/k – 1 + x.
              Exp distribution.

43

Figure 19. Temperature difference for q"/k = 1 + x.
Exp distribution.

44
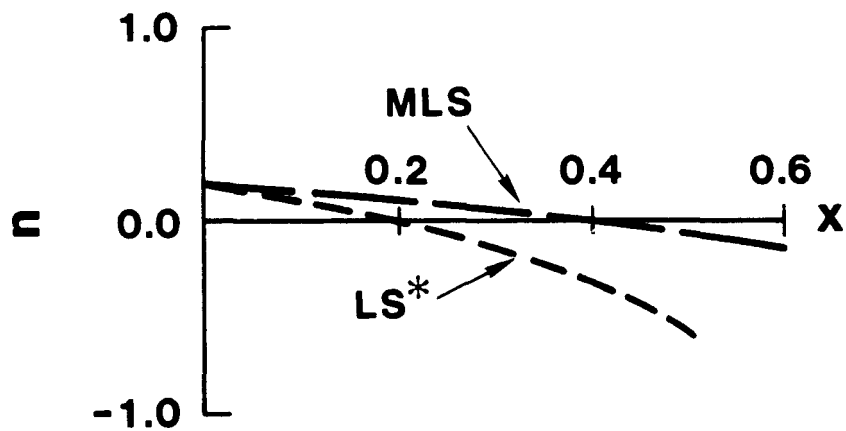
Figure 20a. Variation of n for q″/k — 1 - x.
              PL distribution.
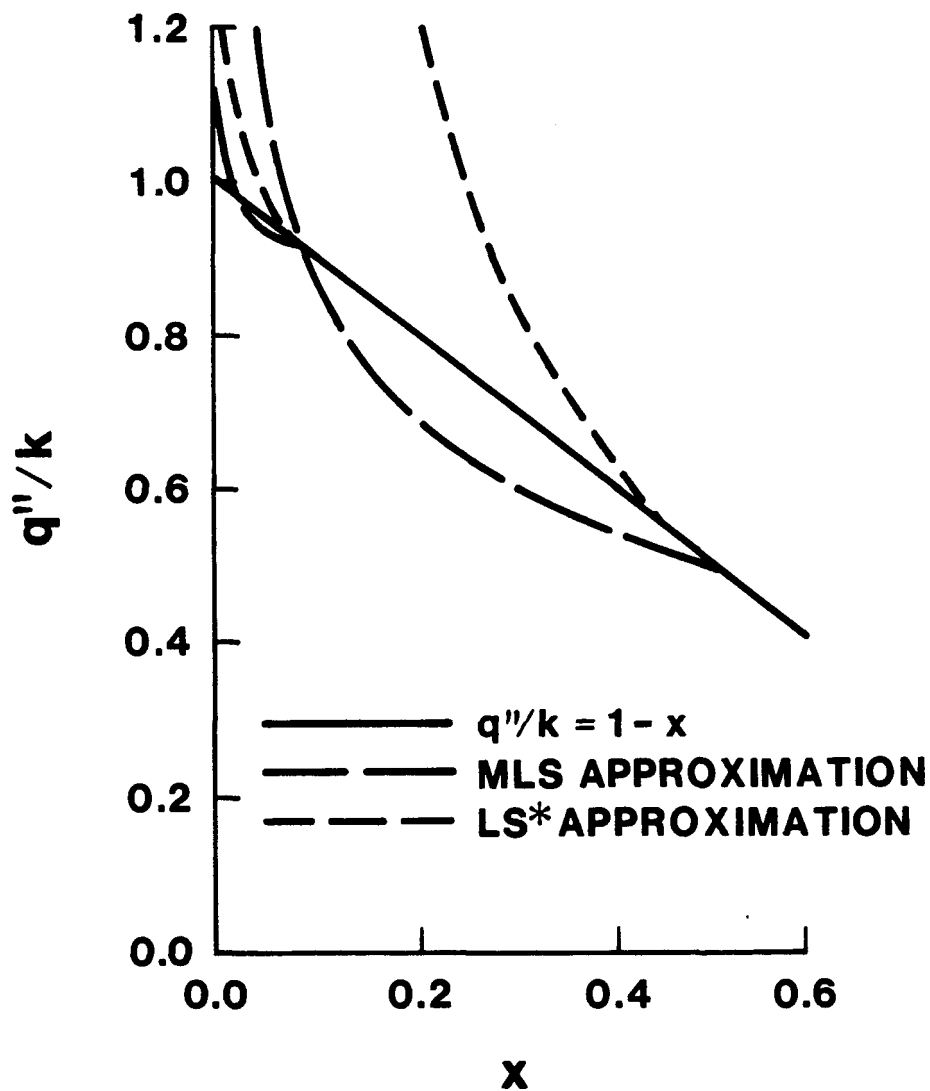
Figure 20b. Approximation of q″/k — 1 - x.
              PL distribution.
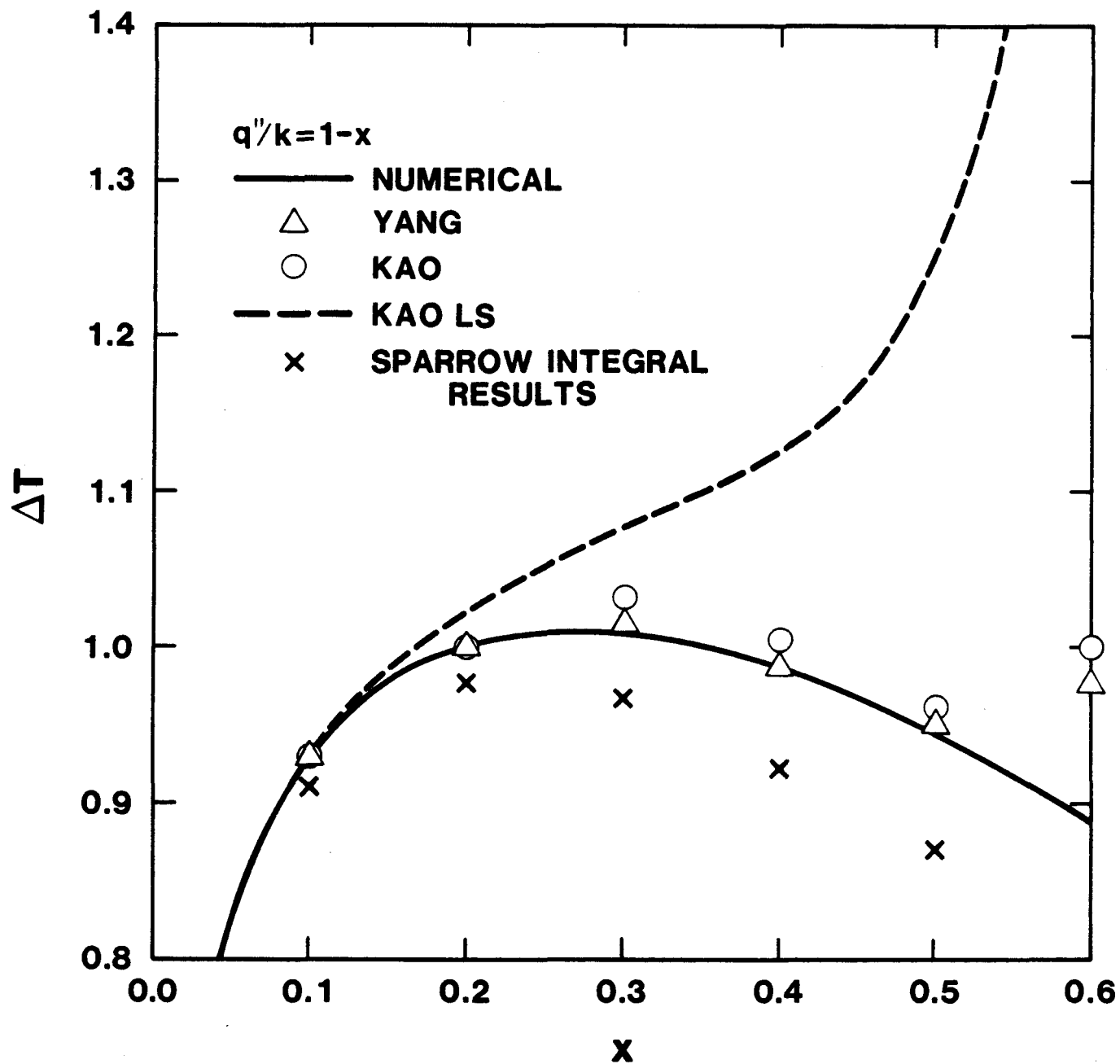
Figure 21. Temperature difference for q"/k = 1 - x.
Results from other methods.
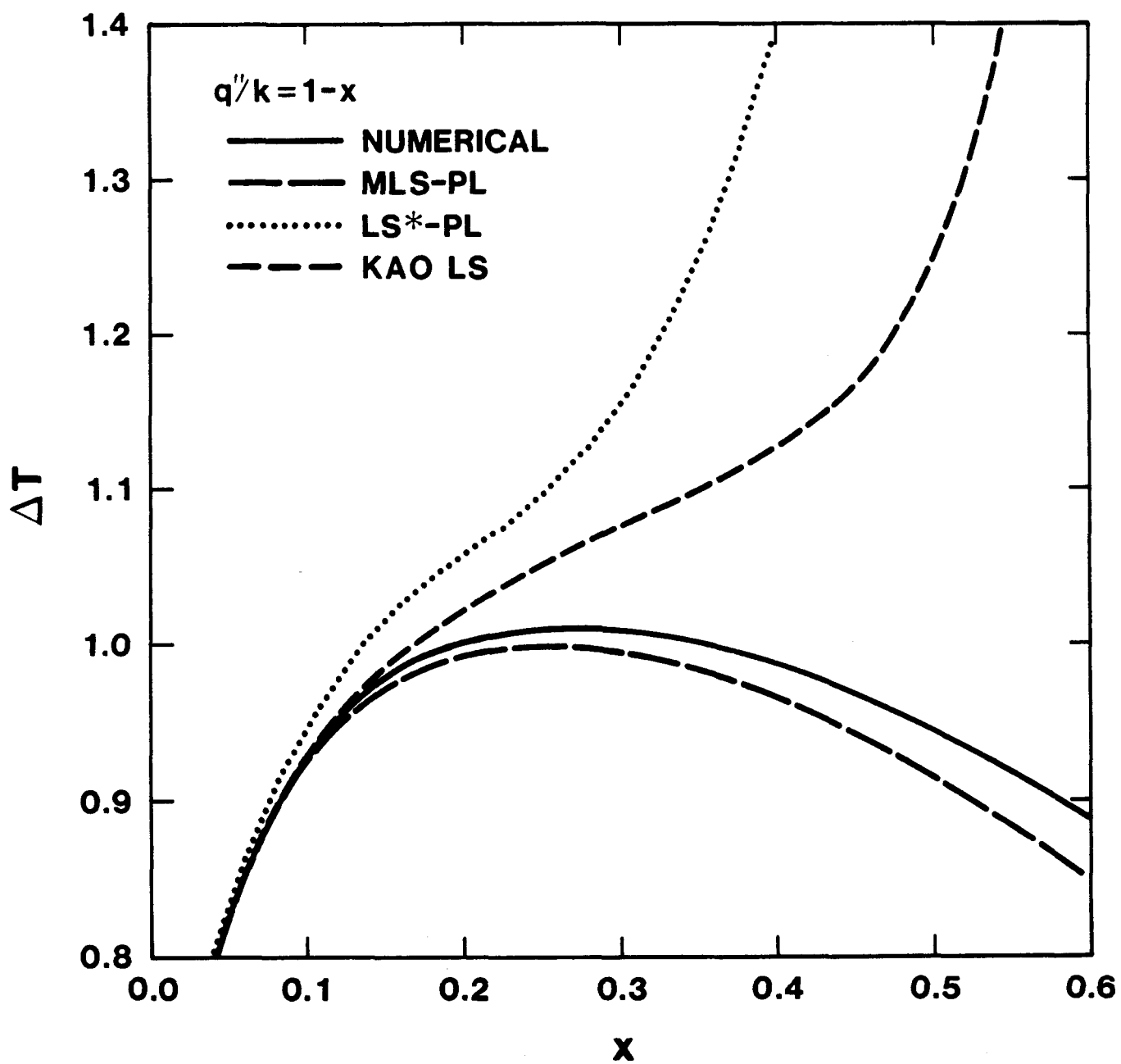
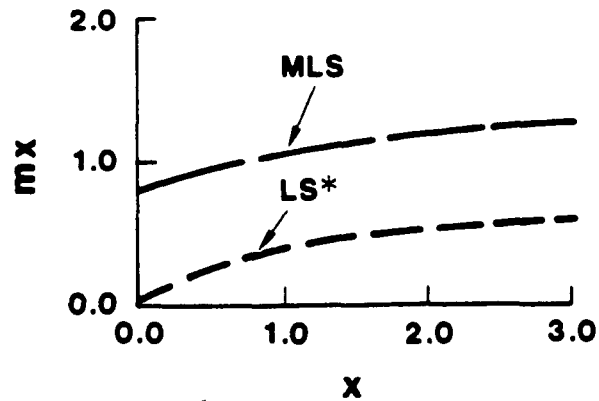Figure 22. Temperature difference for q"/k = 1 - x.
PL distribution.
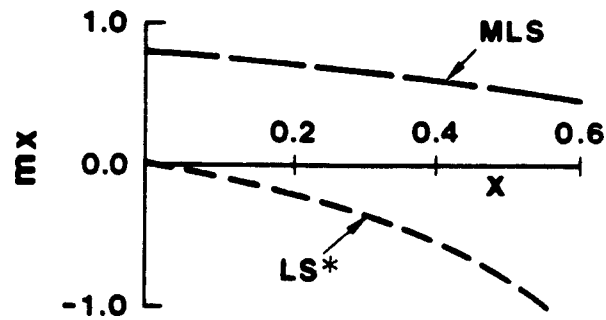
Figure 23a. Variation of mx for q"/k = 1 - x.
Exp distribution.

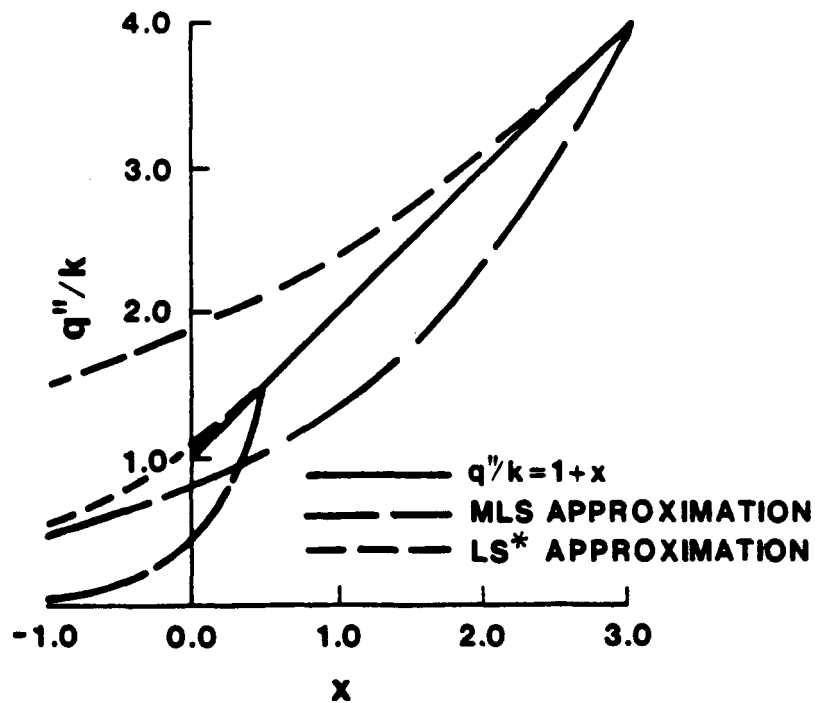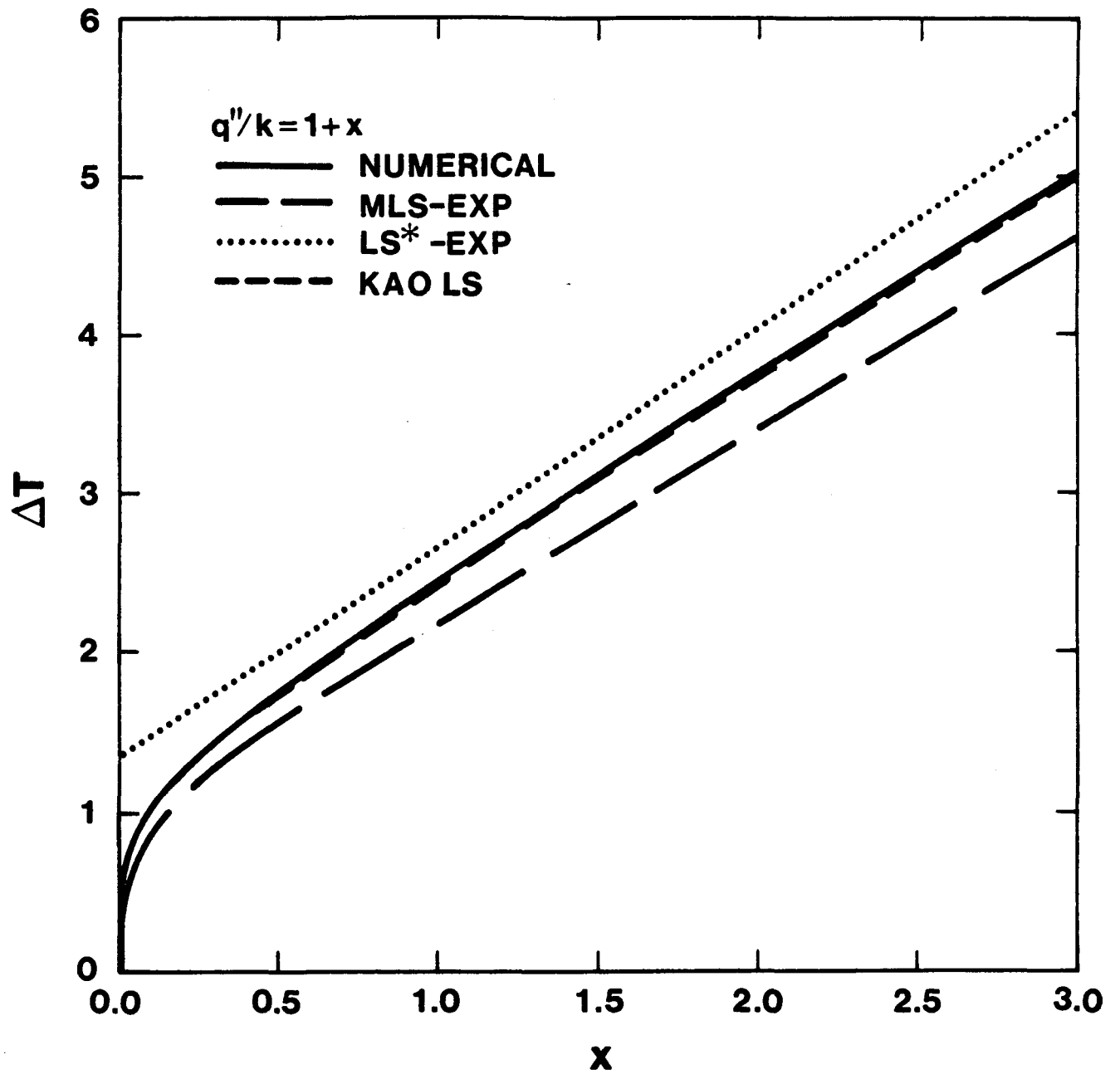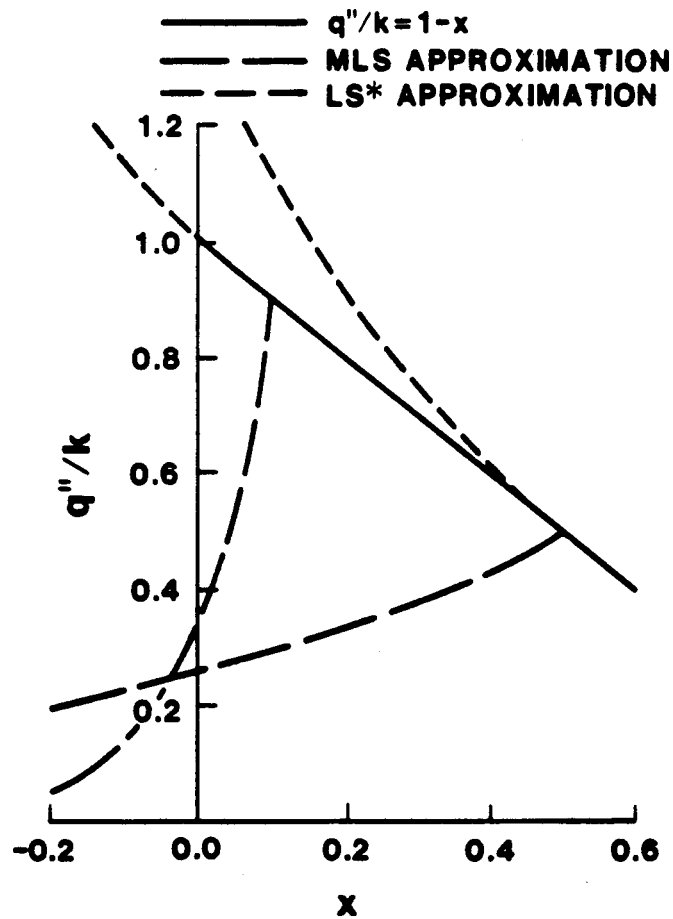Figure 23b. Approximation of q"/k for q"/k = 1 - x.
Exp distribution.

Figure 24 shows the temperature difference predictions for this case. No predictions are available for the LS* approach since the value of mx is less than 0. which, in turn, leads to the fourth root of a negative number. The MLS predictions for this case are surprisingly reasonable, especially considering the poor wall heat flux distribution behavior.
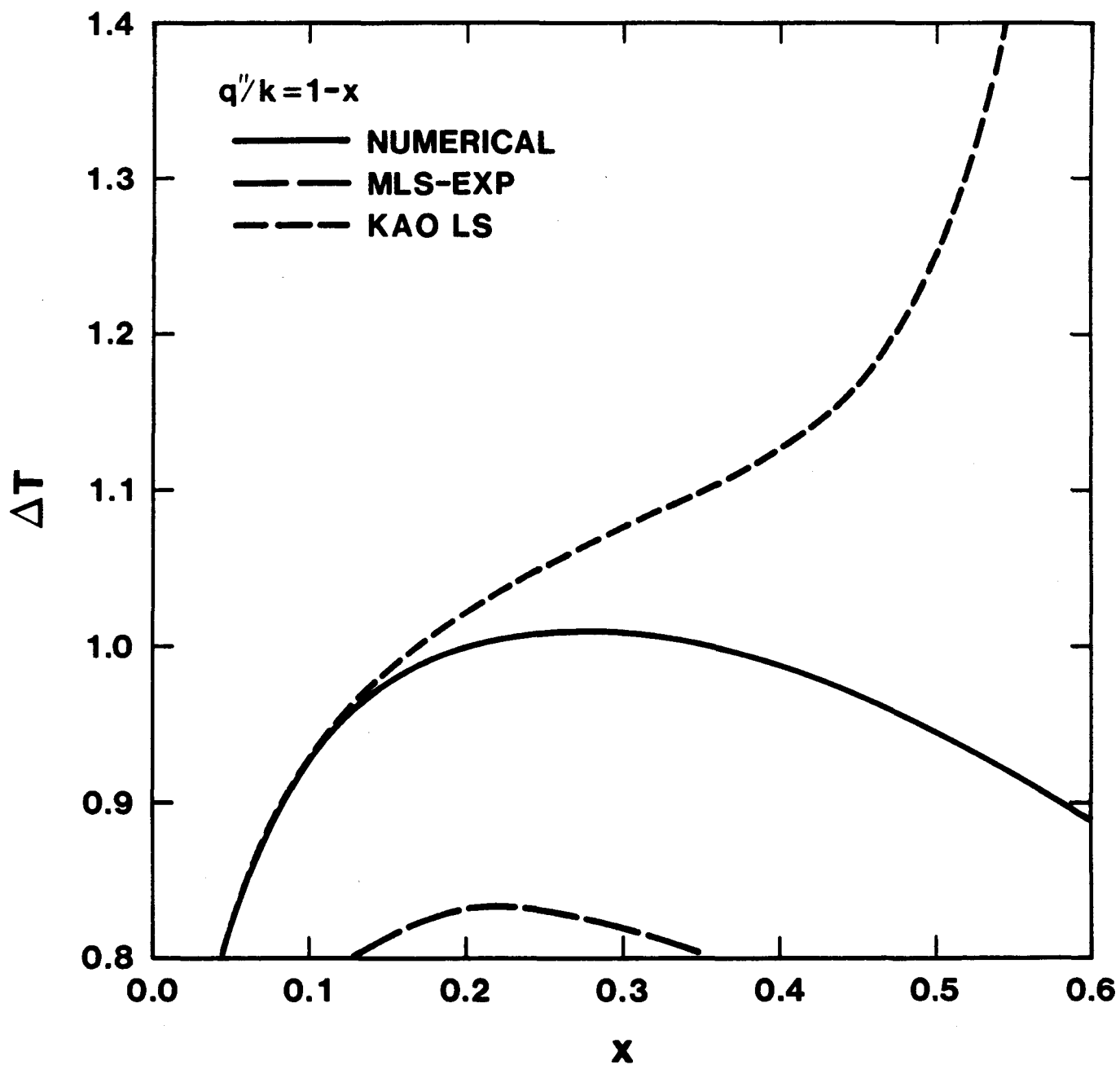
Figure 24. Temperature difference for q"/k = 1 - x. Exp distribution.

B. Stratified Fluid Temperature

The problem under consideration is an isothermal plate in a linearly stratified fluid as shown in Figure 25. The temperature difference between the plate and the fluid decreases linearly with increasing distance up the plate. A similar solution is not available for this problem. Chen and Eichhorn (1976) present a detailed analysis of this problem using local similarity and local nonsimilarity methods for their specific coordinate transformation. Raithby and Hollands (1978) have applied their approximate technique (Raithby, et al. (1975, 1977)) to this problem with good results.

The answers to this problem are given in terms of the ratio of Nusselt numbers for the stratified fluid to that for an isothermal fluid as a function of the stratification parameter S, which is

$$S = \frac{L}{\Delta T} \frac{dT_f}{dx}. \qquad (83)$$

When $S \leq 2$, the entire plate is hotter than the fluid. For $S > 2$, the bottom portion of the plate is hotter than the fluid while the top is colder.

The MLS and LS* approaches have been used to analyze this case for Prandtl numbers of 0.7 and 6.0. For the LS* approach, the value of n is determined by matching the local temperature difference value and the local slope; the value of J was calculated by the appropriate fluid temperature variation equation.

Power-Law Distribution   Figure 26 shows the variation of the similarity parameters n and J along the plate for the MLS and LS* methods and a Prandtl number of 6.0. The results for a Prandtl number of 0.7 are not significantly different and are not shown. For both methods, the value of n decreases with increasing distance along the plate. The change is much faster for the LS* case. The value of J increases along the plate in the MLS method. In contrast, J decreases with increasing distance in the LS* approach.

Figure 27 gives the variation of the temperatures for an x value of 0.5. For both methods, the reference value of the fluid temperature, T_r, is calculated by matching the temperatures at an x value of 0.5. The temperature variation for the MLS method seems a little more reasonable than for the LS* approach in that the temperature difference behavior is closer to the desired variation.

Figure 28 shows the predicted value of the average Nusselt number for a stratified fluid over that for an isothermal fluid with the same average temperature difference for a Prandtl number of 6.0. The MLS predictions are
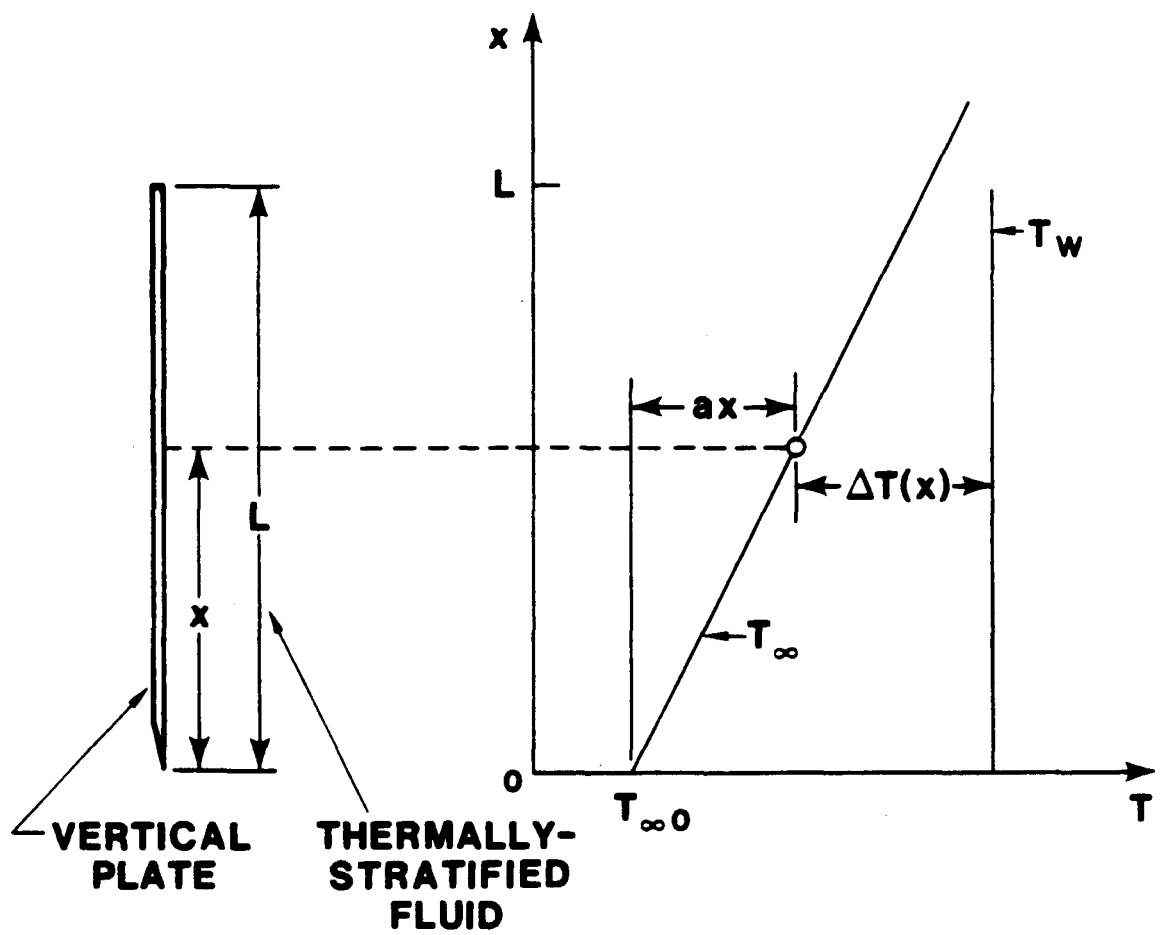
Figure 25. Stratified fluid temperature problem.

Figure 26a. Variation of n for Stratified Fluid Case.
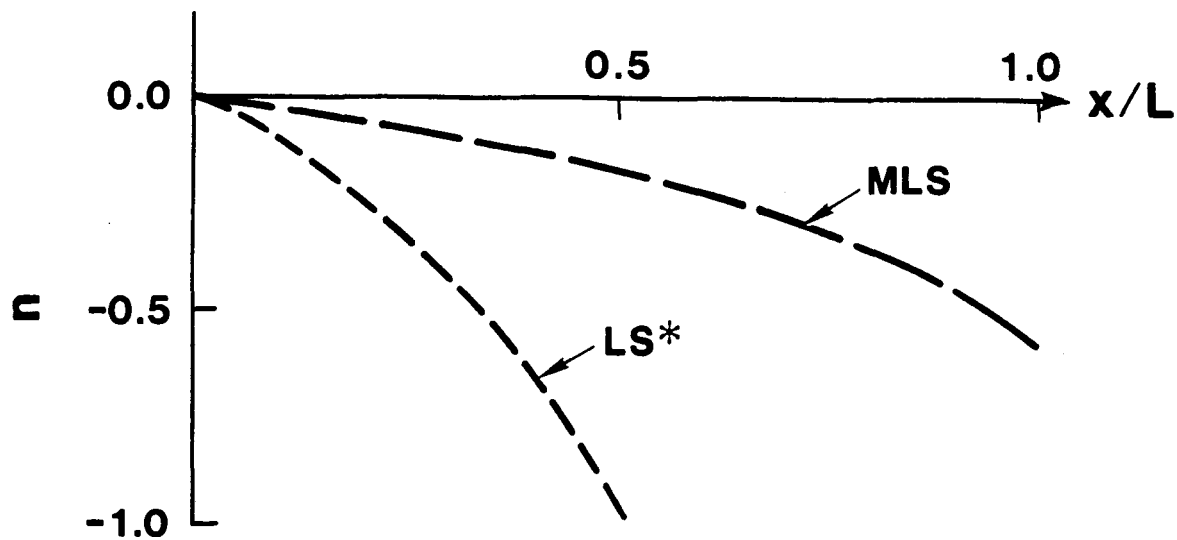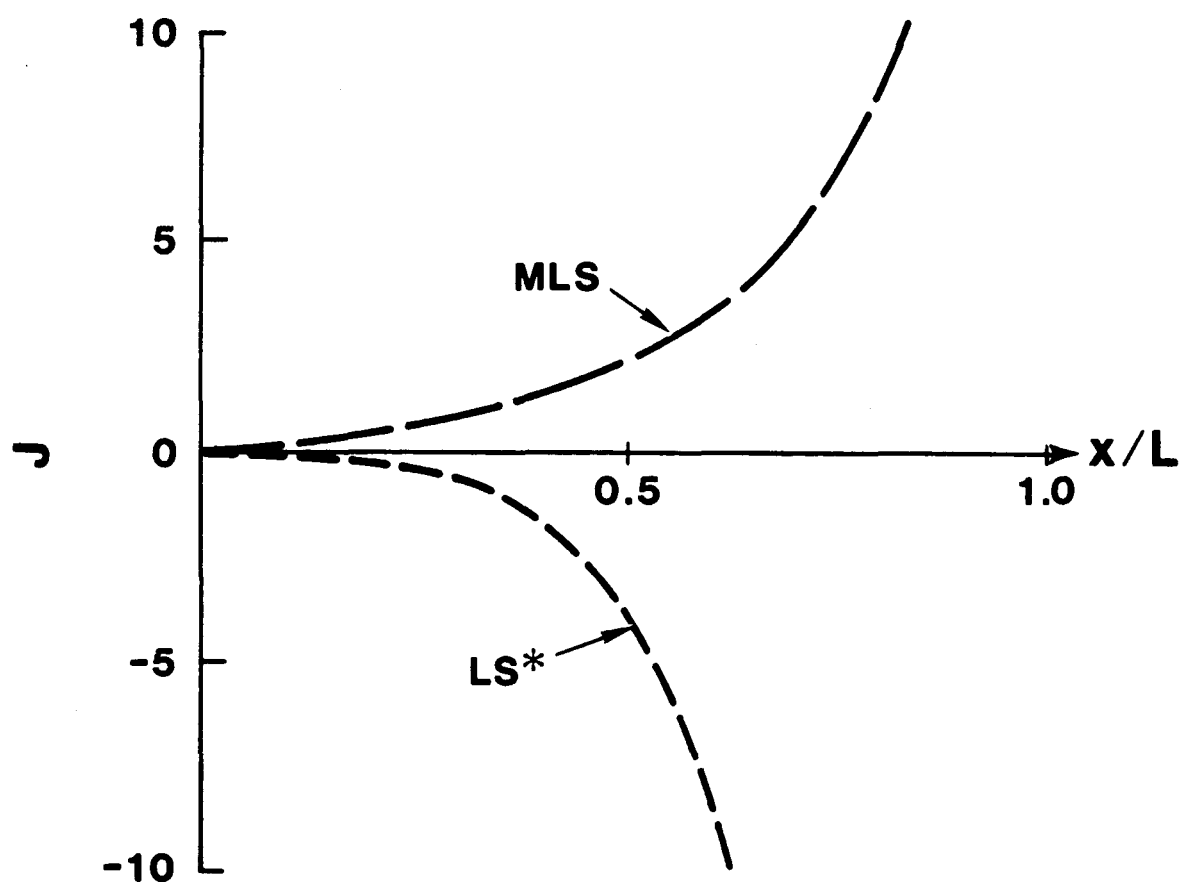PL distribution (S=2).

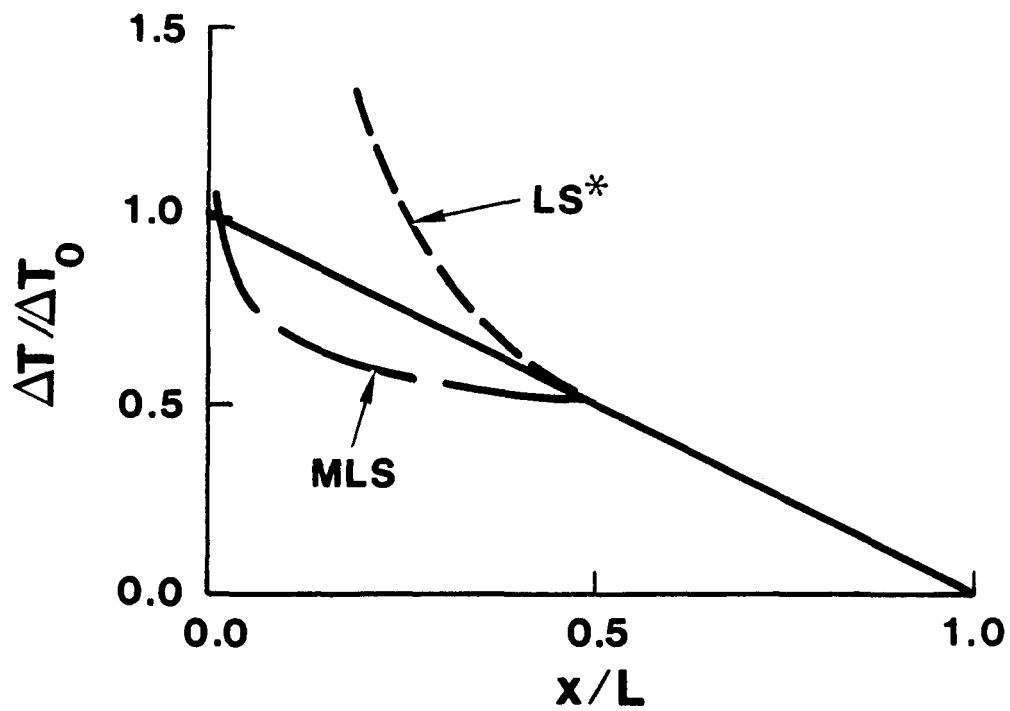Figure 26b. Variation of J for Stratified Fluid Case.
PL distribution (S=2).

Figure 27a. Approximation of ΔT for Stratified Fluid Case.
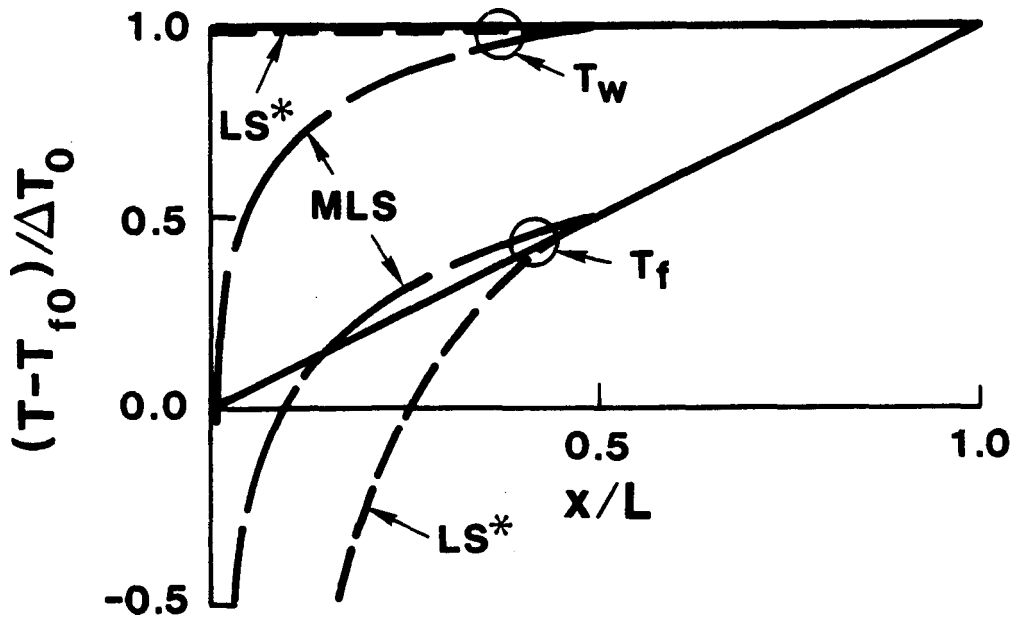PL distribution (S=2).

Figure 27b. Approximation of T_w and T_f for Stratified Fluid Case.
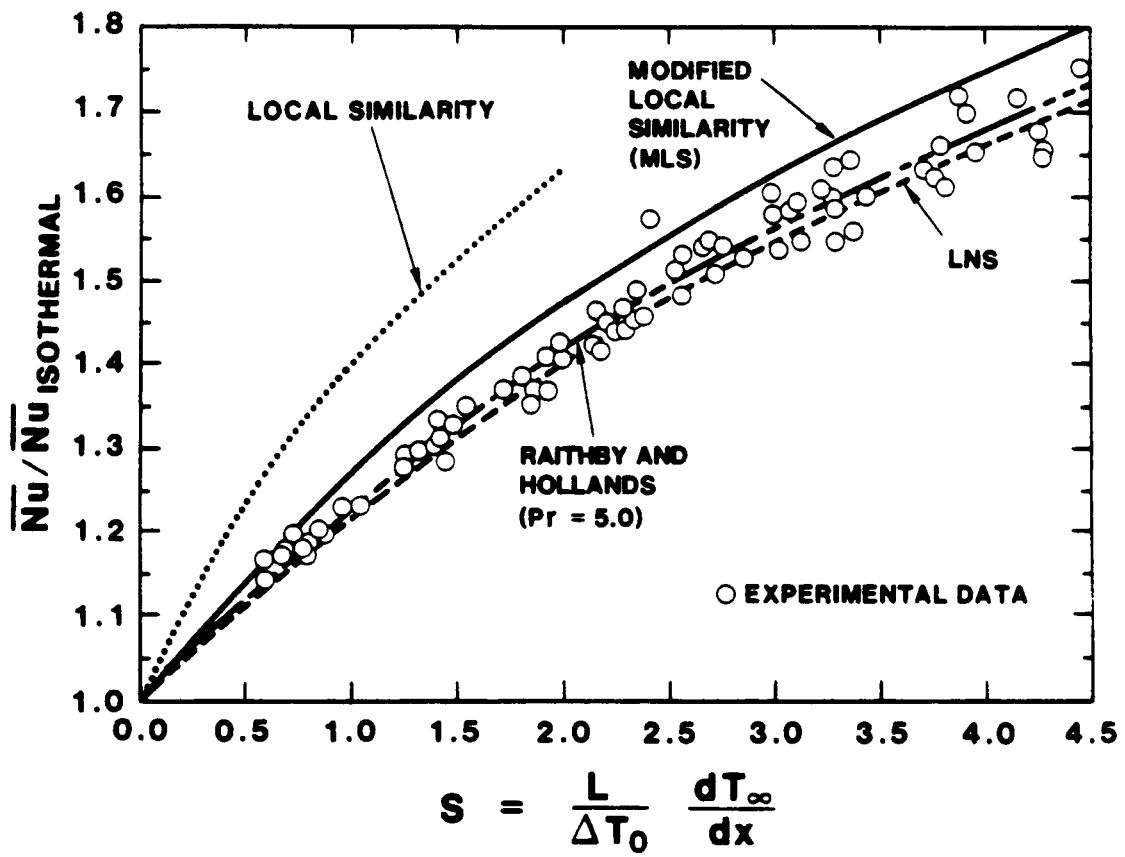PL distribution (S=2).

54

Figure 28. Variation of Nusselt Number with Stratification for Pr=6.0.
PL distribution.

shown on this figure; results from the LS* method are not included as discussed below. The local similarity and local non-similarity (LNS) results are shown as well as the experimental data from Chen and Eichhorn (1976). The predictions by Raithby and Hollands (1978) are also included in the figure.

The MLS results were calculated for a number of discrete S values out to 2.0. For S>2, the predictions are based on an $S^{1/4}$ dependence as used by Chen and Eichhorn (1976) and Raithby and Hollands (1978). The MLS predictions show reasonable agreement with the data with a consistent overprediction of about 4%. The local similarity results by Chen and Eichhorn (1976) are much higher than the data with an error of about 16%. The Raithby and Hollands predictions go right through the data, although their results are for a Prandtl number of 5.0, not 6.0. The LNS results show good agreement with the data with a small consistent underprediction. Overall, the MLS, Raithby and Hollands, and LNS results are in good agreement with the data. The maximum difference between these methods is about 5%, while the uncertainty in the data is of this order, or ±3.2% for Nu and ±3.5% for S (Chen and Eichhorn (1976)).

The LS* method performs poorly for this case. For a Prandtl number of 6.0 and an S value of 2., the wall is always as hot or hotter than the fluid. The LS* method predicts that the wall temperature gradient will change sign about 1/4 up the plate. For the first 1/4 of the plate, heat is transferred from the hotter wall to the fluid. However, for the last 3/4 of the plate, heat is predicted to flow from the colder fluid to the hotter plate, which is unreasonable. Therefore, the LS* predictions are not shown on the figure.

The predictions from the various methods for a Prandtl number of 0.7 are given in Figure 29; no data are available for this case. The MLS method predicts a small decrease (~1%) in the Nusselt number ratio when the Prandtl number is decreased from 6.0 to 0.7. The other methods predict an increase in the ratio of about 5% for Raithby and Hollands to 10% for the LNS approach. Unfortunately, no data are available for this case.

Since the MLS method and the Raithby and Hollands approach are approximations, the LNS results are probably the most accurate. However, some discrepancies have been noted in the Chen and Eichhorn predictions for a Prandtl number of 0.7. Specifically, the numerical results given by Chen and Eichhorn (1976) do not match the values plotted by Raithby and Hollands (1978) or by Chen and Eichhorn (1979). The results used in this report are from Chen and Eichhorn (1979).
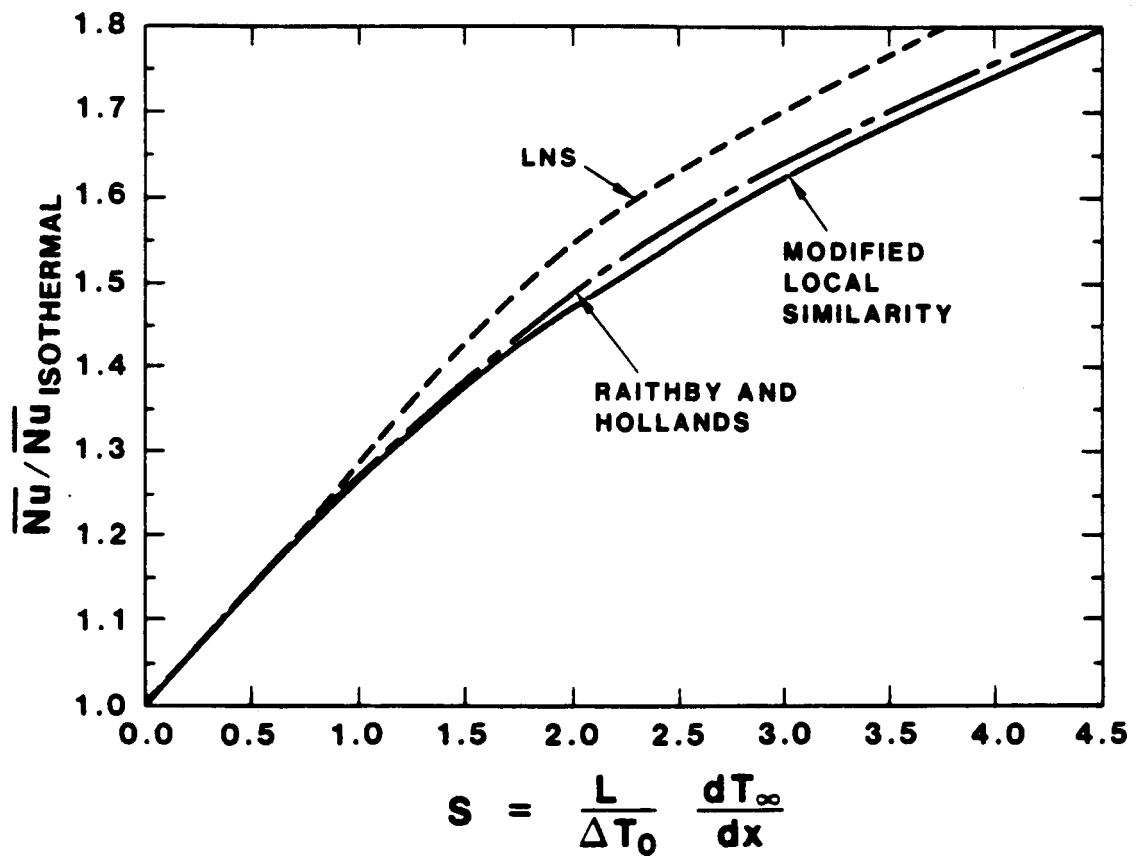
Figure 29. Variation of Nusselt Number with Stratification for Pr=0.7. PL distribution.

Exponential Distribution   Figure 30 shows the variation of the similarity parameters mx/L and J along the plate for the MLS and LS* approaches for a Prandtl number of 6.0. As for the power-law distribution, the results for a Prandtl number of 0.7 are not shown since the results are similar. For both approaches, the value of mx/L decreases along the plate, while the J value increases. However, the values and the signs of both similarity parameters are significantly different for the two approaches as can be seen from the figure.

The variations of the various temperatures are shown in Figure 31 for both methods for an x value of 0.5. The trends exhibited by the LS* approach seem to be superior to those given by the MLS method. The MLS method gives a poor variation of the temperature difference since an increasing temperature difference is predicted while the actual temperature difference decreases along the plate. In contrast to the power-law LS* results, the wall temperature could not be held constant due to the form of the fluid temperature variation equation.

The average Nusselt number variation is depicted in Figure 32 for a Prandtl number of 6.0. For a Prandtl number of 6.0, the MLS results are significantly below the data by about 6%. Results from the LS* method are not shown since, as in the case of a linearly decreasing heat flux, the model blows up for negative values of mx/L. The LNS and the Raithby and Hollands predictions are superior to the MLS approach with the exponential distribution. Figure 33 shows the same results for a Prandtl number of 0.7. The trends are the same as for the higher Prandtl number in that the MLS results are much lower than the other two methods. However, unlike the power-law MLS results, the predicted Prandtl number dependence is similar for all three approaches.
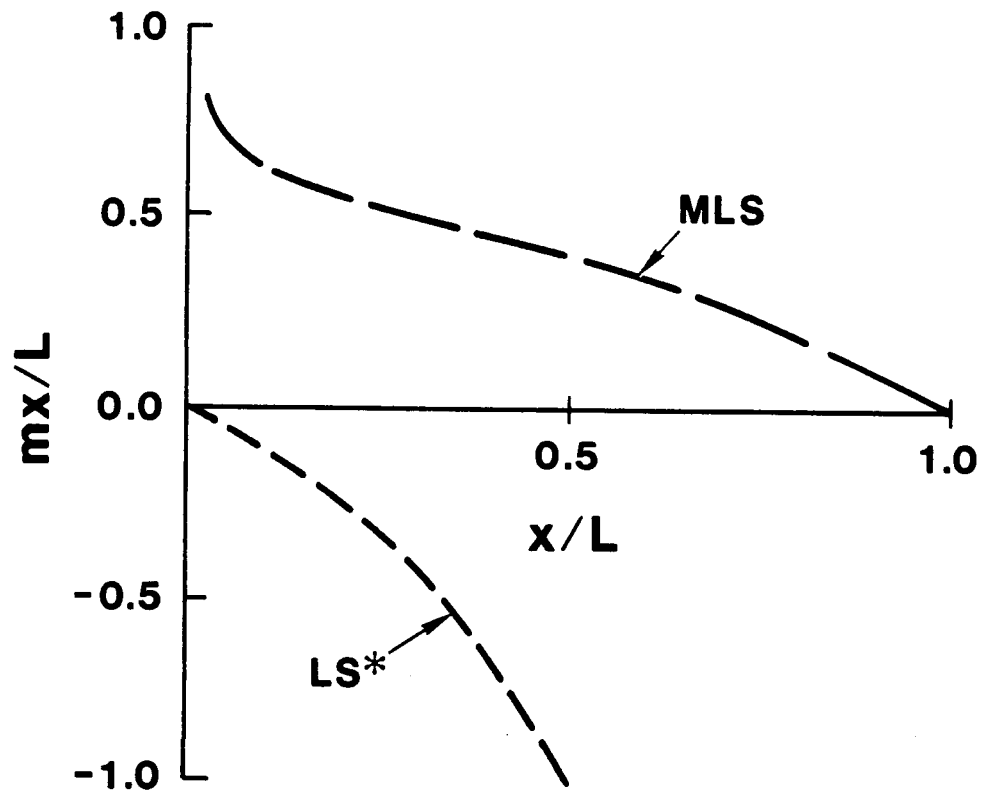
Figure 30a. Variation of mx for Stratified Fluid Case.
Exp distribution (S=2).

Figure 30b. Variation of J for Stratified Fluid Case.
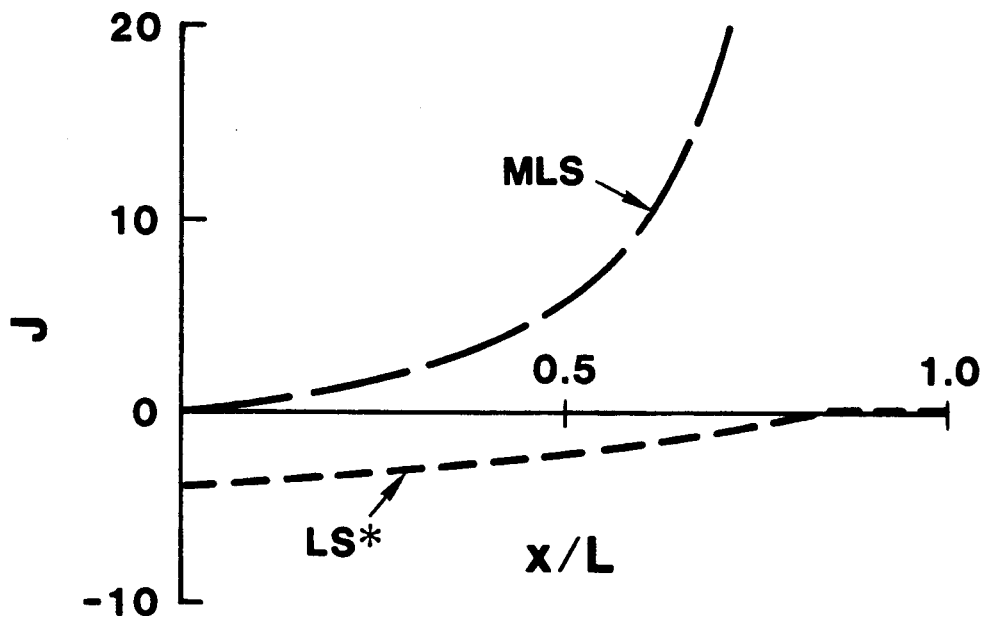Exp distribution (S=2).
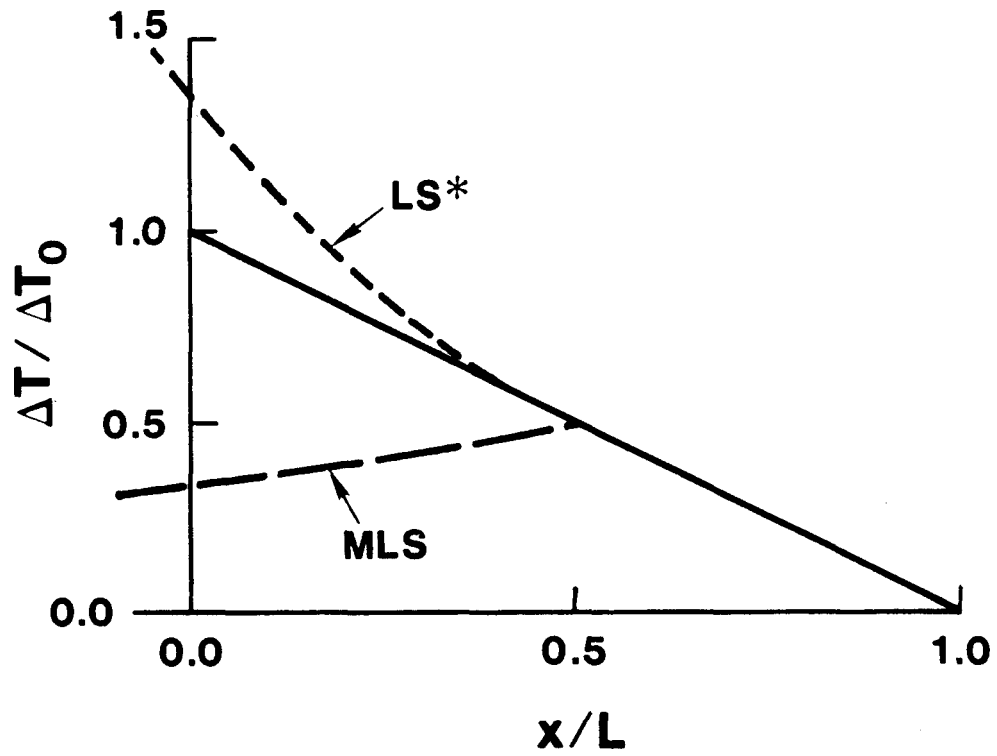
Figure 31a. Approximation of ΔT for Stratified Fluid Case.
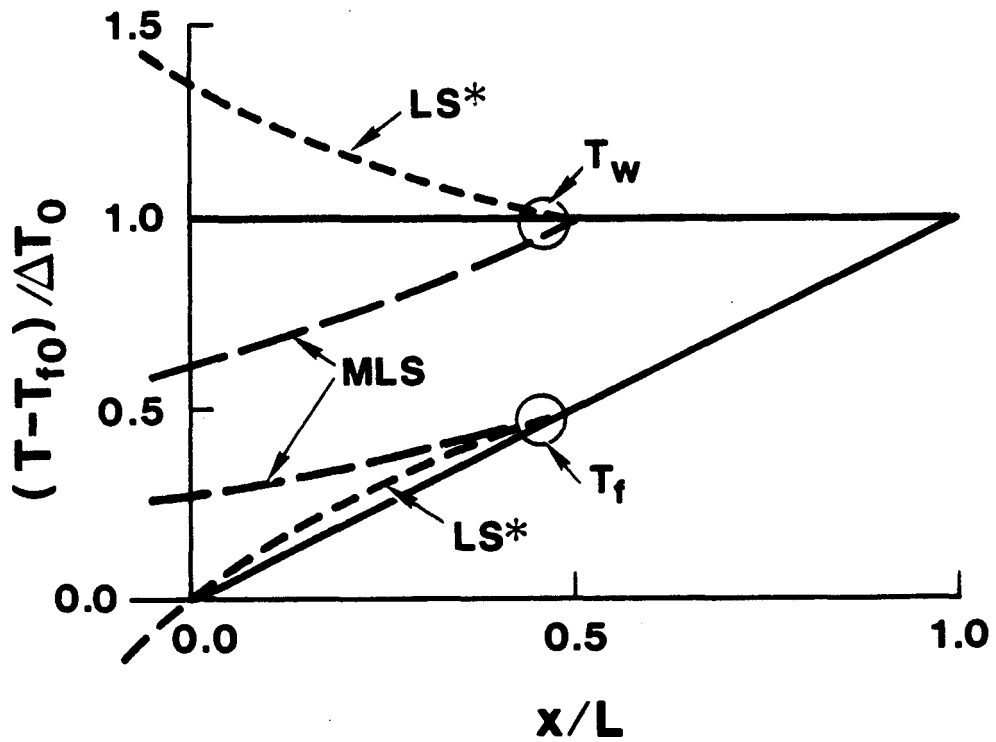Exp distribution (S=2).

Figure 31b. Approximation of T_f and T_w for Stratified Fluid Case.
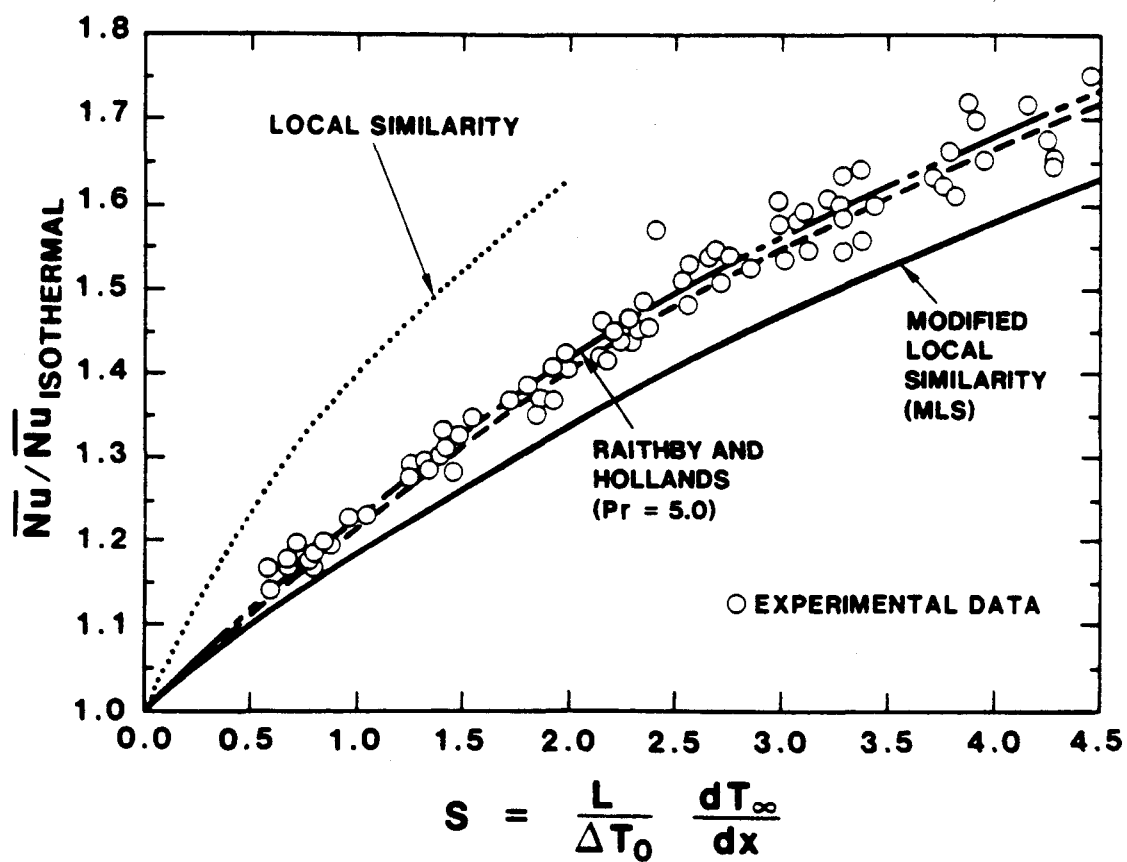Exp distribution (S=2).

Figure 32. Variation of Nusselt Number with Stratification for Pr=6.0.
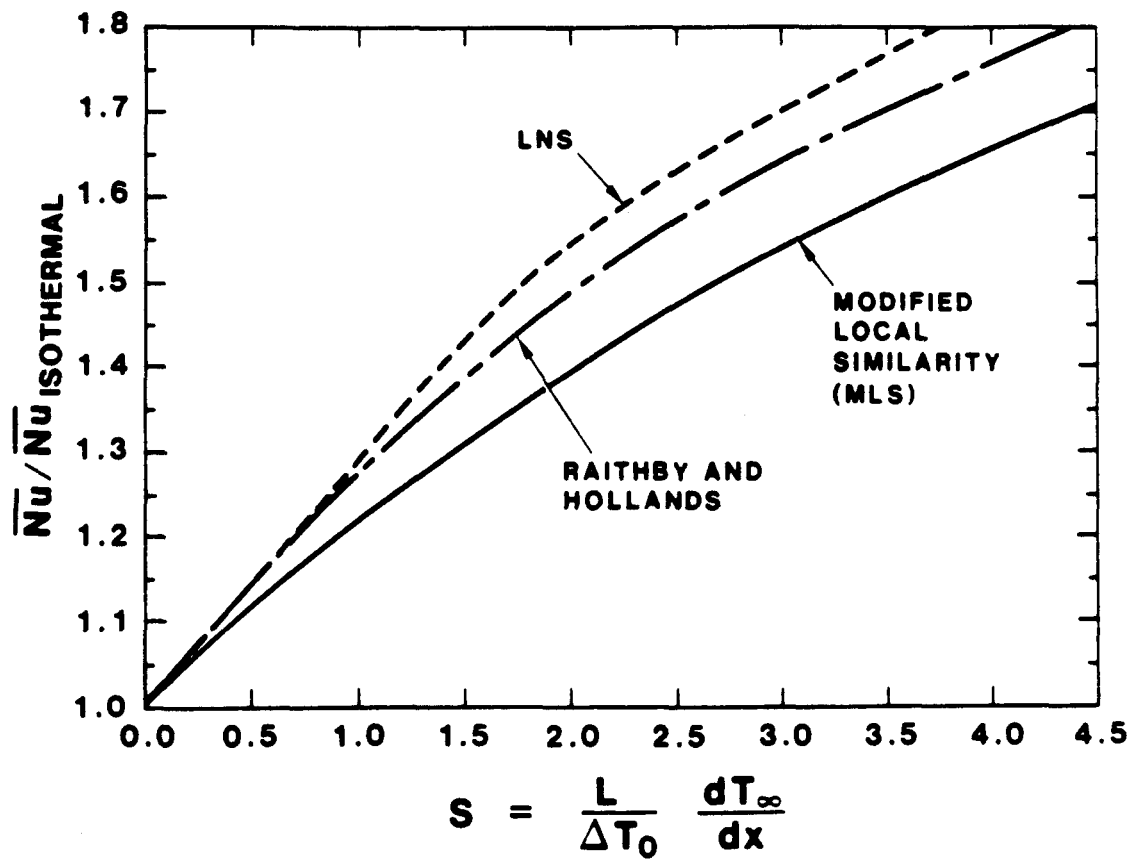Exp distribution.

Figure 33. Variation of Nusselt Number with Stratification for Pr=0.7. Exp distribution.

IV. Discussion

The MLS method has been developed and evaluated for a number of nonsimilar temperature and heat flux cases for the power-law and exponential similarity distributions. For variable conditions where an exact similarity solution does not exist, the MLS method provides an estimate of "equivalent" similarity conditions including velocity and temperature profiles. This estimate is achieved by requiring conservation of energy and the same local heat flux at position x_2. In addition, another possible application of the local similarity approach has been evaluated. The MLS and LS* results have been compared to those from a number of other methods, including a numerical approach. In general, the power-law distribution performs much better than the exponential distribution. The exponential distribution cannot adequately simulate a decreasing temperature difference case, and the non-zero temperature difference at the leading edge is a problem as noted in the disagreement in all cases at x=0., even for those which result in the similarity solution.

This problem with the exponential distribution is not unexpected. As discussed by Sparrow and Gregg (1958) and evaluated by Gebhart and Mollendorf (1969), the results for the exponential distribution are only reasonable if mx_2 is much greater than 1. The reason for this limitation is that the exponential distribution has non-zero values of the boundary layer thickness, momentum, and energy flow at x=0., or at the leading edge of the plate, so the results will only be reasonable if the leading edge contributions are small. In the present case, the values of mx_2 range from much less than 1. to slightly greater than 1. Therefore, in addition to problems in approximating the heat flux profiles, the small mx_2 values are expected to lead to poor comparisons with the correct solutions.

The predictions from the LS* approach vary from reasonable to absurd, so the LS* method is not a reliable technique. In contrast, all the MLS predictions are reasonable even where the more complex methods fail or no longer apply. Through the introduction of global conservation of energy, the MLS method has significantly improved the predictive capability of the local similarity approach.

The MLS method is not without its problems. For specified temperature cases, iteration is required which violates the local similarity assumption. However, in most practical cases, temperatures and heat fluxes are related through heat conduction in the wall, and the more convenient variable can be used. Use of the heat flux information permits use of the MLS method on a local basis consistent with the local similarity approach. The MLS method is not the most accurate approach as expected. However, the method is superior to the traditional local similarity approach. Many of the other more complex approaches, such as the methods of Kao, et al. (1977) and of Yang, et al. (1982), have problems with certain cases such as the linearly decreasing heat flux situation and have not been applied to a nonuniform fluid temperature case. In contrast, the MLS method gives reasonable predictions for all the cases considered. The MLS method is a useful approximate tool for natural convection analysis for analyzing vertical plates for nonsimilar conditions.

V. Summary and Conclusions

The Modified Local Similarity (MLS) method has been developed and applied to natural convection along a vertical flat plate with varying surface conditions and stratification. The MLS approach combines global conservation of energy with the traditional local similarity method for boundary layer profiles. The power-law distribution MLS results are reasonable in all cases evaluated, even where other more complex analytical methods fail or no longer apply. In conclusion, the MLS method is a useful approximate tool for analyzing natural convection on vertical plates for nonsimilar conditions.

Where computing times are a major constraint, such as in the analysis of natural convection in SPR caverns, standard techniques such as finite differences and local nonsimilarity are impractical. In this case, the approximate results provided by the MLS method should provide reasonable results within the computing time constraints. The method has been used in the development of the SPR velocity model as summarized by Webb (1988).

VI. Nomenclature

c_p	specific heat
Exp	Exponential Distribution
f	local similarity variable in the stream function
g	gravitational constant
Gr_m	Grashof number based on m
Gr_x	Grashof number based on x
J	stratification similarity parameter
LS	local similarity
m	temperature difference similarity parameter
$\dot{m}$	mass flow rate
n	temperature difference similarity parameter
N	temperature difference constant
N_a	stratification constant
PL	Power Law Distribution
Pr	Prandtl number
q''	heat flux
Q	integrated heat flux
ΔT	temperature difference, $T_w - T_f$
T	temperature
u	x-direction velocity
v	y-direction velocity
W	width of plate
Δx	difference in x, $x_2 - x_1$
x	distance along plate surface
y	distance normal to plate surface
α	thermal diffusivity
$\tilde{\beta}$	Kao parameter (see appendix)
β	coefficient of thermal expansion
δ	boundary layer thickness
ψ	stream function
η	dimensionless coordinate
μ	viscosity
ν	kinematic viscosity
ρ	density
θ	dimensionless temperature
ξ	dimensionless distance for stratified fluid case

Subscripts

1	value at position x_1
2	value at position x_2
f	fluid
r	reference
w	wall
∞	value at edge of boundary layer

Superscripts

-	average value
'	derivative with respect to η
*	entrainment or ejected value

VII. References

Cebeci, T., and P. Bradshaw (1984), <u>Physical and Computational Aspects of Convective Heat Transfer</u>, Springer-Verlag, New York, 1984.

Chen, C. C., and R. Eichhorn (1976), "Natural Convection From a Vertical Surface to a Thermally Stratified Fluid," Trans. ASME, J. Heat Transfer, pp. 446-451, August 1976.

Chen, C. C., and R. Eichhorn (1979), "Natural Convection From Spheres and Cylinders Immersed in a Thermally Stratified Fluid," Trans. ASME, J. Heat Transfer, pp. 566-569, August 1979.

Gebhart, B. (1985), "Similarity Solutions for Laminar External Boundary Region Flows," <u>Natural Convection - Fundamentals and Applications</u>, edited by S. Kakac, W. Aung, and R. Viskanta, pp. 3-35, Hemisphere Publishing Corporation, Washington, 1985.

Gebhart, B., and J. Mollendorf (1969), "Viscous dissipation in external natural convection flows," J. Fluid Mech., Vol. 38, Part 1, pp. 97-107, 1969.

Jaluria, Y. (1980), <u>Natural Convection Heat and Mass Transfer</u>, Pergamon Press, Oxford, 1980.

Kao, T-T (1976), "Locally Nonsimilar Solution for Laminar Free Convection Adjacent to a Vertical Wall," Trans. ASME, J. Heat Transfer, pp. 321-322, May 1976.

Kao, T-T, G. A. Domoto, and H. G. Elrod, Jr. (1977), "Free Convection Along A Nonisothermal Vertical Flat Plate," Trans. ASME, J. Heat Transfer, pp. 72-78, February 1977.

Lee, S., and M. M. Yovanovich (1987), "Laminar Natural Convection From a Vertical Plate With Variations in Wall Temperature," ASME HTD-Vol. 82, Convective Transport, ASME Winter Annual Meeting, pp. 111-119, December 13-18, 1987, Boston, MA.

Lee, S., and M. M. Yovanovich (1988), "Laminar Natural Convection From a Vertical Plate With Variations in Surface Heat Flux," ASME HTD-Vol. 96, ASME Proceedings of the 1988 NHTC, Vol. 2, pp. 197-205, July 24-27, 1988, Houston, TX.

Minkowycz, W. J., and E. M. Sparrow (1974), "Local Nonsimilar Solutions for Natural Convection on a Vertical Cylinder," Trans. ASME, J. Heat Transfer, pp. 178-183, May 1974.

Raithby, G. D., and K. G. T. Hollands (1975), "A General Method of Obtaining Approximate Solutions to Laminar and Turbulent Free Convection Problems," <u>Advances in Heat Transfer</u>, Vol. 11, Academic Press, 1975.

Raithby, G. D., and K. G. T. Hollands (1978), "Heat Transfer by Natural Convection Between a Vertical Surface and a Stably Stratified Fluid," Trans. ASME, J. Heat Transfer, pp. 378-381, May 1978.

Raithby, G. D., K. G. T. Hollands and T. E. Unny (1977), "Analysis of Heat Transfer by Natural Convection Across Vertical Fluid Layers," Trans. ASME, J. Heat Transfer, pp. 287-293, May 1977.

Sparrow, E. M. (1955), "Laminar Free Convection On a Vertical Plate With Prescribed Nonuniform Wall Heat Flux or Prescribed Nonuniform Wall Temperature," NACA TN 3508, July 1955.

Sparrow, E. M., and J. L. Gregg (1958), "Similar Solutions for Free Convection From a Nonisothermal Vertical Plate," Trans. ASME, pp. 379-386, January 1958.

Sparrow, E. M., H. Quack, and C. J. Boerner (1970), "Local Nonsimilarity Boundary-Layer Solutions," AIAA J. Vol. 8, No. 41, pp. 1936-1942, November 1970.

Sparrow, E. M., and H. S. Yu (1971), "Local Non-Similarity Thermal Boundary-Layer Solutions," Trans. ASME, J. Heat Transfer, pp. 328-334, November 1971.

Webb, S. W. (1988), Development and Validation of the SPR Cavern Fluid Velocity Model, SAND88-2711, October 1988.

Webb, S. W. (1989), Calculation of Natural Convection Boundary Layer Profiles Using the Local Similarity Approach Including Turbulence and Mixed Convection, SAND report in preparation.

Yang, J., D. R. Jeng, and K. J. DeWitt (1982), "Laminar Free Convection From a Vertical Plate With Nonuniform Surface Conditions," Numerical Heat Transfer, Vol. 5, pp. 165-184, 1982.

Yang, K. T. (1960), "Possible Similarity Solutions for Laminar Free Convection on Vertical Plates and Cylinders," Trans. ASME, J. Applied Mech., pp. 230-236, June 1960.

Appendix

Kao Method

The Kao (1976,1977) approach for natural convection is based on a coordinate transformation to lessen the dependence on the streamwise coordinate. The stream function and similarity variables are

$$\psi = \frac{4 \, C_1 \, \nu \, \xi^{3/4}}{P(x)^{1/2}} \, f(\xi, \kappa) \tag{A-1}$$

$$\theta = \frac{T - T_f}{P(x)} \tag{A-2}$$

$$\xi = \int P(x) \, dx \tag{A-3}$$

$$\kappa = C_1 \, P(x)^{1/2} \, \frac{y}{\xi^{1/4}} \tag{A-4}$$

$$C_1 = \left(\frac{g \, \beta}{4 \, \nu^2} \right)^{1/4} \tag{A-5}$$

and, for specified wall temperature variation,

$$P(x) = T_w(x) - T_f \tag{A-6}$$

while for specified heat flux conditions,

$$P(x) = Q^{2/3} \left(\frac{5}{6} \int Q^{2/3} \, dx \right)^{1/5} \tag{A-7}$$

$$Q(x) = \frac{q''(x)}{C_1 \, k}. \tag{A-8}$$

Kao, et al. (1977) state that, for power-law distributions of wall temperature or heat flux, the above transformations reduce to the similarity cases presented by Sparrow and Gregg (1958). However, for the exponential distribution, the two forms are not equivalent. The similarity solution shown by Kao, et al. (1977) for the exponential wall temperature and heat flux cases is just an asymptotic value applicable as $x \to \infty$.

The transformed boundary layer equations are (Kao, et al. (1977))

$$f''' + (3 - 2\tilde{\beta})ff'' - f'^2 + \theta = 4\xi \left(f' \frac{\partial f'}{\partial \xi} - f'' \frac{\partial f}{\partial \xi}\right) \qquad (A-9)$$

$$\frac{\theta''}{Pr} + (3 - 2\tilde{\beta}) f\theta' - 4\tilde{\beta}f\theta = 4\xi \left(f' \frac{\partial \theta}{\partial \xi} - \theta' \frac{\partial f}{\partial \xi}\right) \qquad (A-10)$$

where

$$\tilde{\beta} = \frac{\xi}{P(x)^2 \, dP(x)/dx} \qquad (A-11)$$

and ' denotes differentiation with respect to κ.

For local similarity, the RHS of the equations are set equal to 0., and the equations become

$$f''' + (3 - 2\tilde{\beta})ff'' - f'^2 + \theta = 0 \qquad (A-12)$$

$$\frac{\theta''}{Pr} + (3 - 2\tilde{\beta}) f\theta' - 4\tilde{\beta}f\theta = 0. \qquad (A-13)$$